MASTER'S FINAL THESIS

TITLE: Follow-up control of brushless DC motor based on FOC algorithm

AUTORS: YILIN JIAO

DATA OF PRESENTATION: Month7, Year2023

SURNAMES: **NAME:**

QUALIFICATION:

PLAN:

DIRECTOR:

DEPARTMENT:

TFM QUALIFICATION

COURT

PRESIDENT **SECRETARI** **VOCAL**

READING DATE:

This Project takes into account environmental aspects: □Yes □No

SUMMARY

The main research content of this paper is based on motor theory, power electronics technology, motor control theory, brushless DC motor research object, based on magnetic field oriented control technology to do further design and research of motor control algorithm.The work completed in this paper is summarized in the following parts:

(1) By referring to a large number of Chinese and English references, this paper summarizes the cutting-edge technology and research hotspots of the motor control system, conducts a comprehensive research and analysis on the origin of the motor, the development history of the controller and the general situation of the motor control strategy. In order to achieve the servo control of the motor, the FOC algorithm is used in this project to output sine wave to drive the motor control system. The angle position information of motor is obtained by encoder.

(2) The core components of the brushless DC motor are introduced, the rotor and stator structure and material selection characteristics of the motor body are introduced, the rotor position detection and the working principle of the electronic commutation circuit are introduced, and the corresponding connecting circuit is built according to the working principle of BLDCM.

(3) The principle and control flow of FOC algorithm are introduced. The coordinate transformation and the analysis and judgment of the sector are explained in detail. In particular, park transform and Clark transform are analyzed in detail, including the related formulas and calculation process are described.

(4) In terms of software design, the features and advantages of the STM32CubeMX integrated development environment are first introduced. The hardware abstraction layer of CubeMX can conveniently select the required pins and automatically generate the initialization program, which greatly simplifies our subsequent code writing work. In addition, the program structure diagram is designed and the realization process is described in detail. At the same time, the main algorithm program function and some relatively important program code in the main function are given, including: duty cycle calculation, electrical angle calibration, speed measurement, etc. The pulse width modulation principle of motor control is introduced, and the program code of PWM pulse output is given. Finally, the realization of lower closed-loop control and PID algorithm is introduced, and then all the designed hardware circuits and hardware devices are connected according to the sequence of signals, and the design and welding of the entire BLDCM hardware circuit is completed, including: The circuit module of IGCMF15F60GA minimum system, the circuit module of power supply circuit and the encoder module of real-time detection of rotor position information play the role of core control. After the experimental platform was built, the KEIL MDK V5 debugger was used to download the compiled program code to the control chip through STLINK V2, and finally the motor was tested to be able to follow up control according to the plan.

The test results show that it is feasible to use the FOC algorithm as the brushless DC motor servo control scheme, the control precision of the brushless DC motor is improved, and the motor fluctuation and noise intensity are suppressed to a certain extent. The brushless DC motor designed and realized in this paper is driven by FOC algorithm to achieve a servo control system, which is completed smoothly. Under the control of the algorithm, the output of the brushless DC motor can be started smoothly, and the speed of the motor can be adjusted without pole or the angle of the

electric machine can be locked while the servo control is completed, and the automatic reset can be achieved when external forces are applied. In addition, in the experiment, the noise generated by the motor is very small, and the one-to-many control makes it more suitable for a wide range of applications in factory production and residential life.

Keywords (maximum 10):

Brushless DC motor	Field orientation control	Vector control	Coordinate transformation
Sector calculation	Software test	Hardware test	

ABSTRACT

The brushless direct current motor has the good speed regulation performance of the DC motor, and can achieve uniform and smooth stepless speed regulation under heavy load. At the same time, compared with the traditional brush DC motor, there is no motor contact caused by brush friction commutation, no power generation and other problems. Therefore, it has been widely concerned by industry workers and scholars. Under normal circumstances, the follow-up control for brushless DC motor is generally square wave control. However, when the square wave control is started, the fluctuation is large and the noise is large, which seriously affects the industrial application environment, which causes a great challenge to the practical application of BLDCM. On the other hand, FOC adopts sine wave control mode, which can start smoothly and mute the whole process, and fundamentally solve the noise problem caused by square wave control. Moreover, this control mode divides the stator current of the motor into excitation current and torque current according to the set relationship. The accuracy and rapidity of speed control are greatly improved. Based on the above situation, the study of brushless DC motor FOC algorithm servo control has important theoretical value and practical significance. This thesis focuses on the follow-up control system of DC brushless motor based on FOC algorithm, and the specific research content is summarized as follows:

Firstly, the thesis introduces the research background and significance of brushless DC motor and its drive control system, focuses on their research status and development trend, and introduces the structure and working principle of brushless DC motor. Then, this thesis introduces the basic control principle of FOC algorithm, expounds the corresponding control theory and coordinate transformation theory in detail, and gives the sector calculation process. The servo control system of BLDCM is designed based on FOC algorithm, and the specific control flow is given. Finally, this thesis uses IGCMF15F60GA as the main controller chip of the control system to build the corresponding hardware experiment platform, and carries out joint debugging and testing of the BLDCM system based on FOC algorithm. The experimental results show that the brushless DC motor using the FOC control algorithm can achieve stable operation, and at the same time, it can also achieve the stepless adjustment of the motor speed or the lock of the electromechanical angle while completing the follow-up control function, and can realize the automatic reset under the application of external force. The noise generated by the motor in the experiment is very small.

Keywords (maximum 10):

Brushless DC motor	Field orientation contr	Vector control	Coordinate transformation
Sector calculation	Software test	Hardware test	

SUMMARY OF FIGURES

GLOSSARY OF SIGNS, SYMBOLS, ABBREVIATIONS, ACRONYMS AND TERMS

Brushless direct current (BLDC)

Brushless direct current motor (BLDCM)

Field oriented control (FOC)

Giant Transistor (GTR)

Metal-Oxide-Semiconductor Field-Effect Transistor (MOSFET)

Insulated Gate Bipolar Transistor (IGBT)

Intelligent Power Module (IPM)

Direct current (DC)

Alternating current (AC)

Analog-to-digital converter (ADC)

CATALOG

INTRODUCTION

With the rapid development of industrial and production equipment automation, DC motor plays an important role in industrial production as a device that converts electrical energy into mechanical energy, and is widely used in electric drive because of its good speed regulation performance. According to the brushless DC motor can be divided into brushless DC motor and brushless DC motor [1], [2]. Among them, brush motor is widely used in the field of motion control because of its excellent torque characteristics. Its brush is fixed on the back cover of the motor through the insulation seat and directly introduces the positive and negative poles of the power supply into the inverter of the rotor, and the inverter is connected with the coil on the rotor, and relies on the polarity alternating change and the fixed magnet on the stator to form a force and turn up. Since the inverter is fixed with the rotor, and the brush is fixed with the stator, the friction between the brush and the slip ring constantly occurs when the motor rotates, resulting in a lot of resistance and heat [3]. Therefore, the mechanical brush used by the brush motor directly leads to its low efficiency and very large loss in application, and will lead to poor motor contact and normal operation, but at the same time, it also has the advantages of simple manufacturing and low cost [4]-[6]. Considering the characteristics of brush motor comprehensively, it is necessary to improve the DC motor with the aim of reducing the influence of brush. In 1917, relevant researchers proposed to replace the mechanical brush of the traditional brushed DC motor with a rectifier switch, that is, to design a brushless DC motor [7]. In 1955, the first transistor commutator line was used to replace the mechanical brush of the brushed DC motor, marking the birth of the modern brushless motor. However, there was no motor rotor position detection device at that time, and the motor had no starting capability [8]. In 1962, TG Wilson and PH Trickey invented the first brushless direct current (BLDC) motor based on solid-state technology, which they called the "DC motor with solid-state commutation". Brushless motors do not require a physical commutator, making them the most popular choice for computer disk drives, robots, and aircraft. They used Hall elements to detect the rotor position and control the winding current commutating, making the brushless DC motor practical, but limited by the transistor capacity at that time, the motor power was relatively small [9]. After the 1970s, with the emergence of new power semiconductor devices (such as GTR, MOSFET, IGBT, IPM), the rapid development of computer control technology, and the advent of high-performance rare earth permanent magnet materials, brushless DC motors have developed rapidly and their capacity has been increasing [10]. Since then, researchers have carried out a deeper study and exploration of BLDCM. In the 1980s, with the development of square wave brushless motors and sine wave brushless DC motors, brushless motors really began to enter the practical stage and developed rapidly [11]. The stator and rotor of the brushless DC motor are interchanged based on the ordinary DC motor. The rotor is a permanent magnet to generate air gap flux, and the stator is an armature composed of polyphase winding. In structure, it is similar to a permanent magnet synchronous motor. The structure of the stator of the brushless DC motor is the same as that of an ordinary synchronous motor or induction motor [12]-[15]. Polyphase winding is embedded in the iron core. These windings can be connected into a star shape or a triangle shape, and are respectively connected to each power switch of the inverter for reasonable commutation [16]-[18]. Brushless DC motors can be divided into two types according to the different back electromotive force and drive current waveform: One is a square-wave Brushless DC Motor BLDCM (Brushless DC Motor) whose back electromotive force and driving current waveform are close to trapezoidal wave, and the other is a sine wave brushless DC motor whose back electromotive force and driving current waveform are sine waves, namely a permanent magnet synchronous motor [19].

Despite the wide variety of motors, BLDCM is the most ideal speed regulating motor available today. It integrates the advantages of DC motor and AC motor in one, both DC motor good adjustment performance, and AC motor simple structure, no commutation spark, reliable operation and easy maintenance. In general, the brushless DC motor has the characteristics of long life, high reliability, large torque, etc., and is widely used in industrial control, automotive, aviation, automation system, medical care equipment and other fields [20]-[25]. In the application of BLDCM, its control mode has been widely concerned. Among them, the most common BLDCM control mode is 120° square wave control mode, which is relatively simple, and has a high voltage utilization rate and good economy. However, when this scheme is used, the operation of BLDCM fluctuates greatly and will produce noise, which is not conducive to practical industrial production applications. In order to make up for the shortcomings of square wave control, it is necessary to explore other alternative control schemes [26]-[29]. Therefore, in order to optimize the speed regulation performance of the motor and promote its stable operation, so that it can be better used in the industrial field, the study of its control system has important theoretical value and practical significance. Based on the above discussion, the following Control scheme of brushless motor based on FOC algorithm is studied in this thesis.

In order to study the reliability and stability of small three-phase BLDCM servo control, this paper aims to design a three-phase brushless DC motor control scheme based on FOC algorithm, and realize the motor control by giving specific electrical parameters and control programs. According to the current market situation and design requirements, IGCMF15F60GA chip is selected as a microcontroller unit. Aiming at stable and reliable start, low noise, high precision and smooth speed regulation, this paper analyzes and studies the related problems in the process of motor start and control, and gives the solutions to these problems. Through simulation verification methods such as STM32CubeMX and KEIL MDK, all aspects of the algorithm design were tested in detail, the unity and accuracy of theoretical analysis and design were verified, and the overall algorithm design was completed. The main research content of this thesis is based on motor theory, power electronics technology, motor control theory, brushless DC motor research object, using magnetic field oriented control for motor control design. The main research contents of this paper are as follows:

(1) The first chapter mainly describes the research background and significance of this topic, and elaborates the research status of brushless DC motor control system in detail, describes the core components of BLDCM system, introduces the main motor body components and materials, rotor position sensor and commutation circuit in detail, and analyzes the development trend of BLDCM.

(2) The second chapter briefly introduces the control theory and implementation process of FOC algorithm, and analyzes and deduces related algorithms. The basic coordinate transformation theory of the algorithm, including clark and park transformation, is introduced in detail, and the division and calculation process of sectors are given.

(3) The third chapter introduces the control flow of FOC algorithm used in BLDCM servo control, and gives the system control block diagram and circuit schematic diagram. Write control algorithms through KEIL MDK, download and test them. The results and process of software testing are analyzed and summarized.

(4) In chapter 4, the software part and hardware part of the motor FOC control algorithm are combined, a specific experimental platform is given, the FOC algorithm is experimentally verified, and the operating performance of the system is tested.

(5) In the last chapter, the theory and experimental verification results of FOC algorithm studied in this paper are summarized, and the follow-up exploration content and research trend are discussed.

1. BRUSHLESS DC MOTOR SYSTEM

In order to explore the applicability of the FOC control scheme, the basic structure and control theory of BLDCM are briefly analyzed in this chapter.

1.1 COMPOSITION AND DEVELOPMENT TREND OF BRUSHLESS DC MOTOR SYSTEM

BLDCM control system is usually composed of motor body, rotor position detection and electronic commutation circuit. Different motor body structures correspond to different driving modes. The controller realizes the operation of the brushless DC motor by detecting the rotor position and combining the corresponding control technology [30].

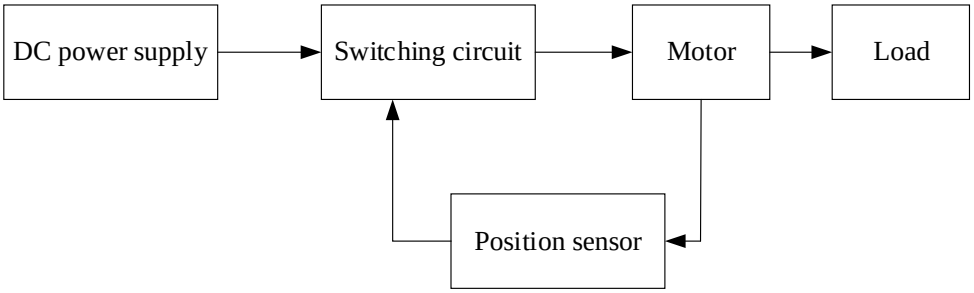

Figure 1. The block diagram of brushless DC motor system

According to the relevant theory, the stator of the brushless DC motor is composed of permanent magnet steel, which can generate a magnetic field in the air gap of the motor, and the reaction magnetic field is generated after the armature winding is energized. When the motor is running, the mechanical brush is commutated, so that the two magnetic fields always maintain a vertical relationship with each other. In this way, the motor will always operate at maximum torque. BLDCM, on the other hand, does not use a mechanical brush for commutation. The stator is installed on the armature winding, and the rotor is installed on the permanent magnetic steel, although the installation mode and the brush DC motor is just inverted, but because BLDCM has no mechanical brush control motor commutation, its armature winding and the magnetic field formed by the permanent magnetic steel can not interact. Therefore, in order to achieve the same effect as the brushed DC motor, the brushless DC motor uses the position sensor and the electronic switching circuit to complete the commutation of the motor, so that the motor runs normally under the action of the torque generated by the interactive magnetic field. The body of BLDCM is mainly composed of stator and rotor. The stator is the stationary part of the motor. It is usually composed of three parts: a stator core, an armature winding and a frame [31]. In order to effectively reduce the stator iron loss, the stator core is generally made of silicon steel sheet laminated. The silicon steel sheet is punched into a ring punch with grooves. At the same time, the surface of the hedge sheet is insulated by moving it to reduce eddy current losses. In order to reduce the torque fluctuation and noise of the motor, the stator core is chute. An electric armature winding can be placed in the slot of the stator. The number of slots needs to consider the number of poles of the permanent magnet and the number of phases of the control circuit. The stator winding is also an important part of the motor body. After the power supply is connected, the current flowing into the winding will generate the corresponding magnetic potential, and then interact with the main magnetic field generated by the rotor permanent magnet to produce electromagnetic torque. When the brushless DC motor is in the state of load operation, a certain back potential will be generated in the winding, and the whole

process of the motor consumes a certain electrical power and outputs mechanical power, converting electrical energy into mechanical energy. The rotor is the rotating part of the motor that generates the main magnetic field and is usually composed of a permanent magnet, a magnetic conductor and supporting parts. Permanent magnets and magnetic conductors are the core of generating magnetic fields. Aluminum nickel cobalt and ferrite are the first and second generation permanent magnet materials used in the early days, and rare earth permanent magnet materials are currently used more. It is mainly divided into rare earth cobalt and NdFeb, characterized by high remanence, high coercivity and high magnetic energy product. However, the magnetic properties of Ndfeb are better and the price is cheaper, so since its advent, it has been widely promoted in industrial and civilian permanent magnet motors. The magnetic conductive material is generally silicon steel, electrical pure iron or 1J50 permalloy. The mechanical supporting parts are composed of a rotating shaft, a shaft sleeve and a pressure ring. They act as fixed permanent magnets and magnetic conductors. As a reliable operation, the shaft needs to withstand a certain strength, so there are usually non-conductive magnetic materials, such as round steel and other grinding. The bushing and pressing ring are usually made of yellow steel and aluminum. The rotor position sensor of brushless DC motor is a key component of brushless DC motor [32]. Its function is to determine the magnetic pole position of the rotor at a certain time, so as to provide the correct signal for the electronic commutation circuit.

The position sensor is usually composed of two parts: the nail and the rotor. The rotor is used to determine the position of the magnetic pole of the motor body, and the stator is placed to detect and output the position signal of the rotor. The sensor has developed so far, and has formed many kinds, which can meet people's different applications. There are three main common, one is the electromagnetic position sensor, its advantage is high strength, can withstand a large impact, while the output signal is large, generally do not need to be amplified can directly drive the switch tube, but its output is AC voltage signal, need to adjust the flow, while the volume is relatively bulky, low signal-to-noise ratio. The second is a magnetic position sensor, which is simple in structure and small in size, and is widely used in occasions where performance and environmental requirements are not high. The last one is the photoelectric position sensor, which outputs DC signal and does not need to be rectified, which is lightweight and reliable, but the signal is weak and needs to be amplified to control the switch tube [33], [34]. In addition to these three common position sensors, position-free sensors have also emerged in recent years. When the motor itself is small and the installation of sensors is inconvenient, this technology can be used, but its starting torque is not high, suitable for use in small motors and light load conditions.

In recent years, position sensors based on Hall elements have also received extensive attention, and have been widely used in motor drives. The type of Hall element belongs to the category of magnetically sensitive sensor. Its working principle in the BLDC system can be summarized as follows: usually the Hall element is installed on the axis of the stator winding, and each phase is installed one, the motor rotor in the process of rotation, the magnetic field will pass through the Hall element, when the Hall element is located in the N pole of the rotor magnetic steel, the Hall electromotive force generated by it is high, and the other is low. Therefore, the position information of the motor rotor can be obtained through the high and low levels of the three Hall electromotive forces.

The electronic commutation circuit of BLDCM is composed of power switching device and logic control circuit. The power switching device distributes the power of the DC power supply to each phase winding of the stator in a certain logical relationship, so that the electric machine continuously generates torque and sends out the output. The control part is to change the signal detected by the sensor into the corresponding pulse

signal to drive the power switch device, so as to realize the function of controlling the on-time of each phase winding of the motor stator.

For BLDCM, the electronic switching circuit is used to control the turn-on time and sequence of each phase winding of the motor stator, which is composed of a power switching unit and a logic control circuit. Among them, the power switching unit is the main part of the entire electronic switching circuit, which is composed of 6 MOSFET transistors. Its role is to distribute the power of the power supply to the phase windings of the motor according to the set relationship, so that a phase of the winding is conductive, thus generating phase current and promoting the rotor of the motor to rotate. At this time, the position sensor captures the position signal of the motor and quickly converts it into the corresponding electrical signal to the logic control circuit. The logic control circuit processes the electrical signal, and produces the corresponding pulse signal to act on the transistor, so that the transistor has the corresponding function. It can be seen that the two parts of the electronic switching circuit interact and complement each other, and they work together to enable the normal operation of the brushless DC motor.

So far, the main switch of BLDCM is generally a full control device such as IGBT or MOS switch, and some main circuits have integrated power modules and intelligent power modules, which can greatly improve the reliability of the system.

Nowadays, with the deepening development of industrial automation and the emergence of new technologies and new materials, the development of BLDCM ontology tends to be miniaturized and integrated. In addition, due to the rapid development of microelectromechanical system technology and control algorithm, the brushless DC motor control system can collect the current signal, voltage signal and speed signal of the motor at the same time, and then feedback the comprehensive signal back to the motor, improving the precision of the motor control system. Different from the brushless DC motor, BLDCM is the use of position sensors to control the motor commutation, it relies on sensors to integrate the motor rotor position information and speed information back to the motor control circuit, the future, with the rapid development of sensor technology and electronic power technology, the degree of intelligence of brushless DC motor will continue to deepen. BLDCM usually adopts 120° square wave control, although the square wave control is relatively simple and easy to operate, it will cause large fluctuations when the brushless DC motor starts, resulting in noise. In addition, the motor will also produce torque pulsation at low speed. Therefore, using sine wave to drive brushless DC motor is a wise choice, the control mode will use space vector pulse width modulation (SVPWM) control, it is more efficient than the general pulse width modulation (PWM) control, and can effectively suppress the motor torque ripple. Therefore, BLDCM control tends to adopt SVPWM control technology to achieve high efficiency of PWM control.

1.2 BRUSHLESS DC MOTOR CONTROL SYSTEM

1.2.1 SQUARE WAVE AND SINE WAVE CONTROL

At present, the control of DC brushless motor includes square wave control and sine wave control. Square wave control is to obtain the position of the motor rotor through the Hall sensor, and then according to the position of the rotor in 360° electrical cycle, 6 reverses (once every 60°). Each commutator position motor outputs a force in a specific direction, so it can be said that the position accuracy of the square wave control is electrical 60°. Because under this control, the phase current waveform of the motor is close to the square wave, it is called square wave control. The drive algorithm

of square wave control scheme is simple, the development difficulty is low, the development cost is low, and the hardware cost is lower than that of chord wave control. In addition, square wave control requires low hall phase, phase inductance and phase resistance of the motor [35]-[39].

Sine wave control uses SVPWM wave, the output is 3-phase sine wave voltage, and the motor phase current is sine wave current. It can be considered that several continuous changes of commutation are carried out in one electrical cycle, without abrupt commutation current [40]. Obviously, sine wave control compared with square wave control, its torque fluctuation is smaller, the current harmonics are less, and the control feels smoother. The sine-wave control scheme runs smoothly and the torque fluctuation is small. Similar to the servo control, the operation effect is smooth, not easy to fluctuate by load changes. And chord wave control is more stable and reliable, high service life, can avoid the impact of peak current, and square wave control is easy to produce peak current, impact on MOS switch and motor, easy to affect the service life. In addition, quiet, low noise, high efficiency, energy saving and emission reduction are the advantages of chord wave control. Accordingly, the algorithm of string wave control is more difficult, and the cost is higher than that of other wave control [41]-[43].

1.2.2 FOC CONTROL

FOC was first proposed by F.Blaschke in Germany in 1971 [44]. After years of development and improvement testing, it has now developed into the most practical servo control system algorithm [45]. FOC has been widely used in the industrial field, and the technology application is very mature. Compared with square-wave drive technology, FOC technology has a very prominent advantage and can fundamentally solve the noise problem existing in traditional square-wave control [46]-[48]. The phase current of the driving motor runs in the form of sine waves, so its torque ripple is small and the noise is small. Because the FOC uses a unique space vector debugging output, when the motor decelerates, the system automatically returns energy to the bus, the motor has an active braking effect, and the deceleration is very fast. In addition, FOC uses mathematical methods to decouple the torque and excitation of the three-phase motor and decompose the stator current of the motor into the excitation current (direct axis current) and the torque current (alternating axis current), making the speed control of the motor accurate and fast [49]. At present, FOC drive technology has been widely used in the power system of multi-rotor unmanned aerial vehicle, which better solves the shortcomings of the existing power system.
FOC control is also called vector control, its basic idea is to select a rotating magnetic field axis of the motor as the set synchronous rotation axis. In brushless DC motor, rotor magnetic field, air gap magnetic field and stator magnetic field are three kinds of rotating magnetic field axes to choose from. However, the coupling between the air-gap magnetic field and the stator magnetic field in the magnetic resonance chain will make the vector control structure elusive. Therefore, it is usually determined that the rotor magnetic field is the FOC controlled synchronous rotation axis. The basic approach is to use the coordinate transformation in mathematics to decompose the sine wave stator current of BLDCM into a magnetic field component current parallel to the magnetic field and a torque component current perpendicular to the magnetic field (these two currents are also called direct axis current and alternating axis current), and control the two currents respectively. In fact, this approach is to decompose the sine wave current into two stable currents, that is, to realize the complete decoupling of the magnetomotive current component and the torque current component, so as to obtain the dynamic performance similar to the square wave drive control. FOC control is mainly composed of Clake transform, Park transform, Park inverse transform, PID control and SVPWM control. In the application, FOC algorithm can be used to realize

the speed control of BLDCM.

To implement FOC control, two input signals must be given. This includes the three-phase current of the motor and the rotor position signal of the motor. Both signals are indispensable. The essential control modules are: The Clarke module (mainly used to convert the collected three-phase motor current signal into the current signal in the stationary coordinate system), the Park module (to convert the current signal in the stationary coordinate system to the synchronous coordinate system d-q), the PI adjustment module of the D-axis and the Q-axis (mainly used to control the speed and maintain the D-axis as 0), and the anti-Park The module (mainly converts the current signal of the synchronous rotating coordinate system d-q to the stationary coordinate system) and the SVPWM module (converts the stationary coordinate system signal into the pulse signal of the control of the drive axle) [50]-[54].

2. THE CONTROL PRINCIPLE OF FOC ALGORITHM

The traditional brushless DC motor often uses 120° square wave drive, but the square wave drive will cause large fluctuations when the motor starts, resulting in noise problems. And sine wave drive can overcome these problems, in recent years more and more widely used, the development is more and more rapid. However, the sine wave drive technology is more complex, because the size of the sine wave changes over a period of time and is difficult to control. FOC is a technology that uses frequency converter to control the three-phase motor, and controls the output of the motor by adjusting the output frequency of the frequency converter and the size and Angle of the output voltage. Because the three-phase output current and voltage will be represented by a vector during processing, it is called vector control. The FOC control technology can decompose the sinusoidal wave whose size changes according to the period into two constant DC waves, which makes the sinusoidal wave drive similar to the square wave drive, thus simplifying the sinusoidal wave drive technology.

2.1 BASIC THEORY OF FOC CONTROL

FOC is also called vector control, its basic idea is to select a rotating magnetic field axis of the motor as a set synchronous rotation axis to control the electromagnetic field direction of the motor. In brushless DC motor, rotor magnetic field, air gap magnetic field and stator magnetic field are three kinds of rotating magnetic field axes to choose from. However, there is coupling between the air-gap magnetic field and the stator magnetic field in the flux linkage relationship, which makes the vector control structure uncertain. Therefore, it is usually determined that the rotor magnetic field is the FOC controlled synchronous rotation axis. The basic approach is to use the coordinate transformation in mathematics to decompose the sine wave stator current of BLDCM into a magnetic field component current parallel to the magnetic field and a torque component current perpendicular to the magnetic field (these two currents are also called direct axis current and alternating axis current), and control the two currents respectively. In fact, this approach is to decompose the sine wave current into two stable currents, that is, to realize the complete decoupling of the magnetomotive current component and the torque current component, so as to obtain the dynamic performance similar to the square wave drive control. The torque of the rotor is proportional to the vector product of the stator's magnetic field vector and the rotor's magnetic field vector. It can be seen from the relationship of vectors that if the torque of the motor is maintained at the maximum time, the stator magnetic field vector should be perpendicular to the rotor magnetic field vector. Because the size and direction of the magnetic field are directly related to the size and direction of the current, the key to controlling the BLDC with the FOC control algorithm is to control the size and direction of the three-phase input current.

The key to control the vertical of stator magnetic field and rotor magnetic field is to control the stable three-phase input voltage and its current vector, and to know the real-time position of the rotor. For the direction control of input current, FOC gives the concept of space current vector. Its essence is to combine the current vector of the three phases, and then decompose into two components perpendicular and parallel to the axis of the rotor magnet, that is, d-q structure. The magnetic field generated by the vertical current component is orthogonal to the magnetic field of the rotor, which creates a rotating torque. The current component parallel to the rotor magnetic axis, the magnetic field generated is consistent with the rotor magnetic field, will not produce any torque. A good control algorithm needs to minimize the current component parallel to the rotor magnetic axis, because this current component will only cause the motor to generate heat and aggravate the wear of the bearing. We need to control the current in

the coil to maximize the current component perpendicular to the rotor magnetic axis.

In order to minimize the stator current vector in the same direction as the rotor magnetic field and maximize the vertical magnetic field, the chord wave current in the stator coil needs to be adjusted in real time with the rotation Angle of the rotor. Control stable three-phase current input can be established PID controller, PID control is constantly modulated input, once the motor current is converted into d-q structure, control will become very simple. We need two P-I controllers; One controls the current parallel to the rotor magnetic field, and one controls the vertical current. Because the control signal of the parallel current is zero, this makes the parallel current component of the motor also become zero, which drives the current vector of the motor to be converted into a vertical current. Since only vertical currents can produce effective torques, the efficiency of the motor is maximized. The other PID controller is mainly used to control the vertical current to obtain the required torque consistent with the input signal. This allows the vertical current to be controlled as required to obtain the desired torque.

There are two situations to determine the real-time position of the rotor: position sensor and no position sensor. For sensors, because the motor sensor (generally the encoder) can feedback the position information of the motor rotor, the position estimation algorithm can be not used in the control, and the control is relatively simple, but for motor applications with sensors, the control performance is often higher. For sensorless, because the motor does not have any sensor, the position information of the motor rotor cannot be obtained by simply reading the measured value of the sensor. Therefore, the position estimation algorithm is used to calculate the rotor position by collecting the phase current of the motor in the control process.

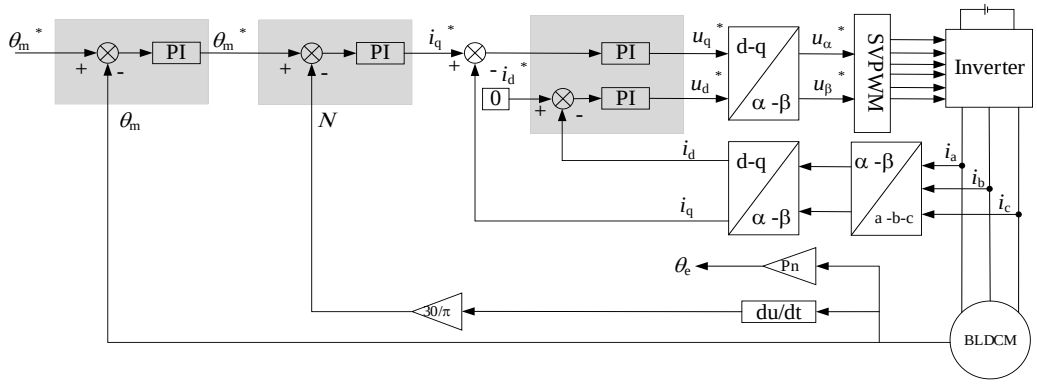

Figure 2. Angle control schematic diagram

Fig. 2 shows the corresponding schematic diagram of Angle control. The specific principle is described as follows:

First, the collected two-phase current is transformed by clark to obtain the quadrature current of two axes, d and q; after rotation transformation, the quadrature current I_d and I_q are obtained, among which I_q is related to torque and Id is related to magnetic flux. In practice, I_d is usually set to 0. These two quantities are not time-varying, so they can be controlled separately. The I_q and I_d values obtained are respectively sent to the PI regulator to obtain the corresponding output uq and ud. The motor rotation Angle is obtained through the sensor, and the inverse park transformation is performed to obtain the current of two axes, d and q. The inverse clark transformation of u_a and u_b is carried out to obtain the actual three-phase voltage input to the inverter bridge to drive the motor rotation.

2.2 COORDINATE TRANSFORMATION THEORY

Considering that the equation of brushless DC motor is complicated, in order to facilitate further research, coordinate transformation theory can be used to deal with it accordingly. The specific implementation principle is: using the coordinate change to transform the motor rotor variables and stator variables into a rotating coordinate system, the coordinate system is the field orientation axis that must be selected to achieve the FOC algorithm, and its rotation angular speed is ω. Fig. 3 shows the basic phasor diagram of the coordinate transformation theory. In Fig. 3, it is assumed that f_{ax}, f_{bx} and f_{cx} are three-phase transient variables, and the Angle between them is 120°.

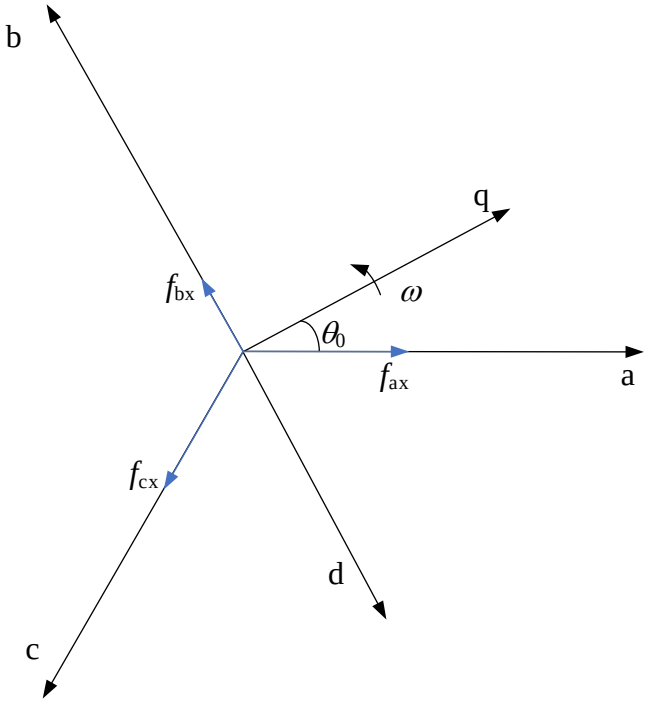

Figure 3. Coordinate transformation phasor diagram

In the abc coordinate system shown in Fig. 3, the three-phase voltages of a,b, and c are as follows:

$$\begin{cases} v_a = \sin(wt) \\ v_b = \sin(wt - 120°) \\ v_c = \sin(wt - 240°) \end{cases} \quad (1)$$

The three-phase voltage of equation (1) is synthesized to obtain a vector:

$$\vec{V} = \sin(wt)e^{i0} + \sin(wt - 120°)e^{i120°} + \sin(wt - 240°)e^{i240°} \quad (2)$$

By simplifying equation (2), equation (3) can be obtained.

$$\vec{V} = \frac{3}{2}(\sin(wt) - \cos(wt)i) \quad (3)$$

Combined with formula (3), equation (4) in the two-phase rest coordinate system can be obtained

$$\begin{cases} V_\alpha = \frac{3}{2}\sin(wt) \\ V_\beta = -\frac{3}{2}\cos(wt) \end{cases} \tag{4}$$

From the point of view of phase Angle, with the same phase, with the phase difference of 90°.
In terms of amplitude, the amplitude of the resultant vector is 3/2 times that of the A-phase voltage. If the constant amplitude transformation is carried out, the amplitude of the two is equal. For A constant power conversion, the resultant vector has an amplitude of sqrt(3/2) times the A-phase voltage.

The corresponding transformation matrix is as follows

$$\begin{bmatrix} U_\alpha \\ U_\beta \\ 0 \end{bmatrix} = \mathrm{m} * \begin{bmatrix} 1 & -\frac{1}{2} & -\frac{1}{2} \\ 0 & \frac{\sqrt{3}}{2} & -\frac{\sqrt{3}}{2} \\ \frac{1}{2} & \frac{1}{2} & \frac{1}{2} \end{bmatrix} \begin{bmatrix} v_a \\ v_b \\ v_c \end{bmatrix} \tag{5}$$

In equation (5), the constant amplitude transformation is when m = 2/3, and the constant power transformation is when m = sqrt(2/3).

The principle of Park transformation is shown in equation (6).

$$\begin{bmatrix} v_\mathrm{d} \\ v_\mathrm{q} \end{bmatrix} = \begin{bmatrix} \cos\phi & -\sin\phi \\ \sin\phi & \cos\phi \end{bmatrix} \begin{bmatrix} v_\alpha \\ v_\beta \end{bmatrix} \tag{6}$$

In formula (6), φ is the angle between U_d and v_α .

Substituting equation (6) into the Clark transformation matrix gives the Park transformation matrix of equation (7).

$$\begin{bmatrix} U_d \\ U_q \\ U_0 \end{bmatrix} = m * \begin{bmatrix} \cos\phi & \cos(\phi - \frac{2\pi}{3}) & \cos(\phi + \frac{2\pi}{3}) \\ -\sin\phi & -\sin\left(\phi - \frac{2\pi}{3}\right) & -\sin(\phi + \frac{2\pi}{3}) \\ \frac{1}{2} & \frac{1}{2} & \frac{1}{2} \end{bmatrix} \begin{bmatrix} v_a \\ v_b \\ v_c \end{bmatrix} \tag{7}$$

From the perspective of phase angle, Park transforms into DC, and there is no phase angle change.

From the perspective of amplitude, under constant amplitude transformation, it can be obtained

$$v_\mathrm{d}^2 + v_q^2 = v_\alpha^2 \tag{8}$$

In a constant power state, it can be obtained

$$v_{\mathrm{d}}^2 + v_q^2 = \sqrt{\frac{3}{2}} v_\alpha^2 \tag{9}$$

It should be noted that the Clark and Park transformations at constant power values have $\varphi_0 = 0$. The conversion process is shown in Fig. 4 and Fig. 5.

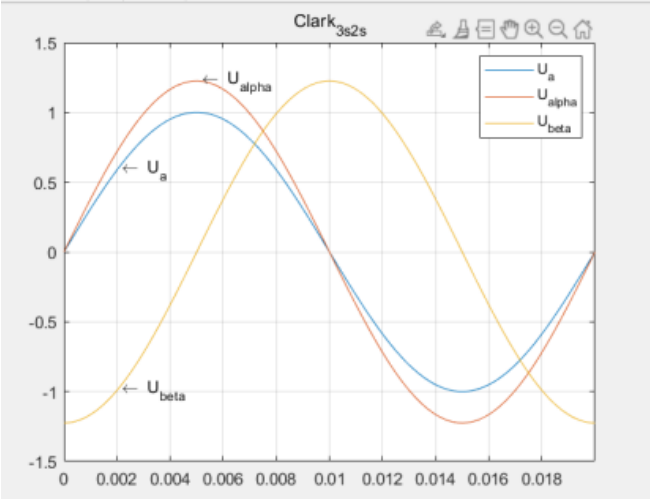

Figure 4. Clark transformation in a constant power state

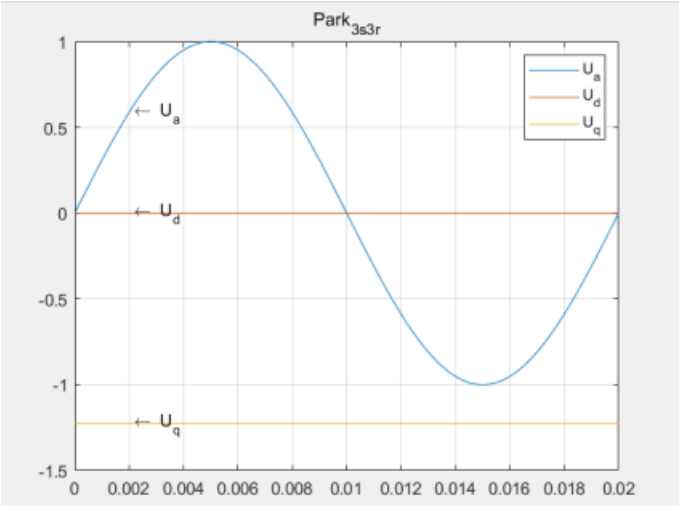

Figure 5. Park transformation in a constant power state

It should be noted that the Clark and Park transformations at a constant amplitude have $\varphi_0 = 0$. The conversion process is shown in Fig. 6 and Fig. 7.

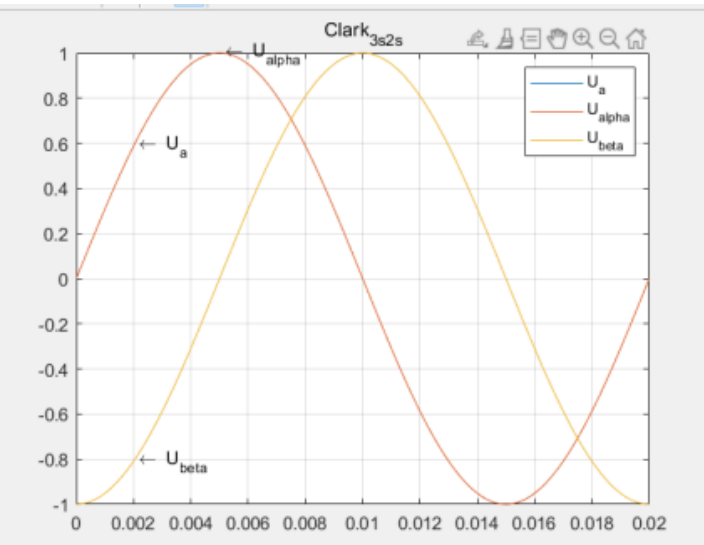

Figure 6. Clark transformation in a constant amplitude state

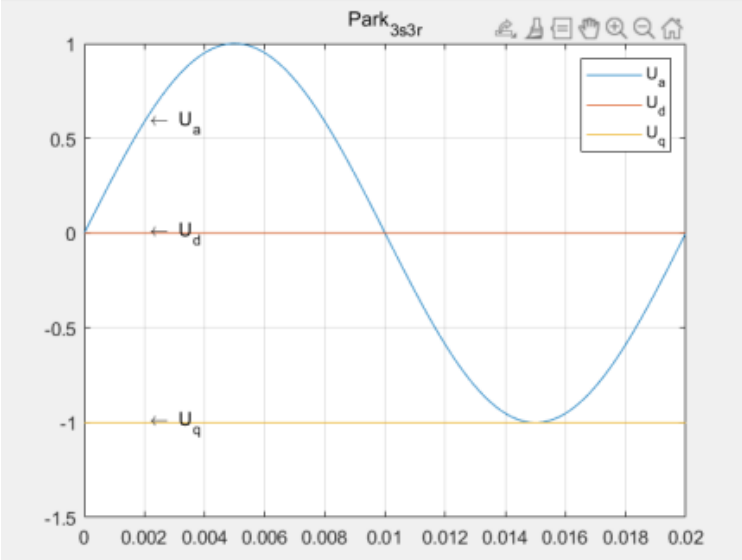

Figure 7. Park transformation in a constant amplitude state

2.3 SECTOR COMPUTATION

In recent years, space voltage vector pulse width modulation (SVPWM) has been widely used in BLDCM control. It is a pulse width modulated wave output by six transistors in a three-phase bridge circuit according to a certain modulation mode, which can realize the approximate sinusoidal phase current waveform of the motor. Therefore, SVPWM modulation is a very core technology in FOC technology. As the core content of vector control, this part gives the sector calculation process. Different from PWM control, SVPWM control is based on the overall effect of the three-phase output voltage to consider, the ideal trajectory of the three-phase synthetic total voltage is a circle, in SVPWM control, the actual magnetic flux formed by the various switch combinations of the inverter to approximate this circle, and then obtain higher control performance. The theoretical basis of SVPWM control is the average equivalent

principle, that is, in a given period, select several vectors as reference vectors, and then use these reference vectors to synthesize the vectors we need in space. For the brushless DC motor, we take the voltage vector as the reference object, that is, through the average equivalent principle, we finally get a space voltage vector whose trajectory is close to the circle. Then the switching state of the inverter is determined by comparing it with the ideal space voltage vector locus, and the corresponding pulse modulation waveform is generated. Fig. 8 is a three-phase bridge inverter circuit. The following is a mathematical derivation of the basic principle of SVPWM control based on the structure diagram.

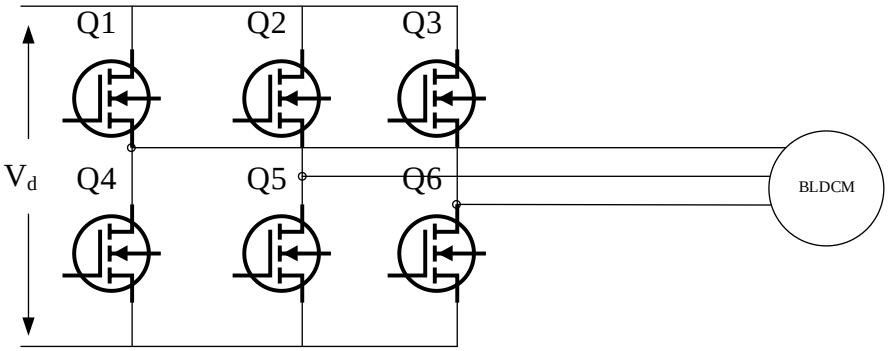

Figure 8.The structure diagram of the inverter

In Fig. 8, it is taken into account that one of the inverter structures has six pipes, which have two working states, namely on and off. Now assume that when the upper bridge arm is conducting, the switch state is 1, and conversely, when the lower bridge arm is conducting, the switch state is 0. The vector synthesized by the vector of the force generated by the three-phase electricity moves in a uniform circular motion around the origin, and taking into account the opposite conduction state of the two switches on each bridge arm, the three-phase bridge voltage inverter has 8 operating states, which are represented by vectors. Six non-zero vectors U_1(001), U_2(010), U_3(011), U_4(100), U_5(101), U_6(110) and two zero vectors U_0(000), U_7(111). Fig. 9 shows the corresponding voltage sector vector diagram.

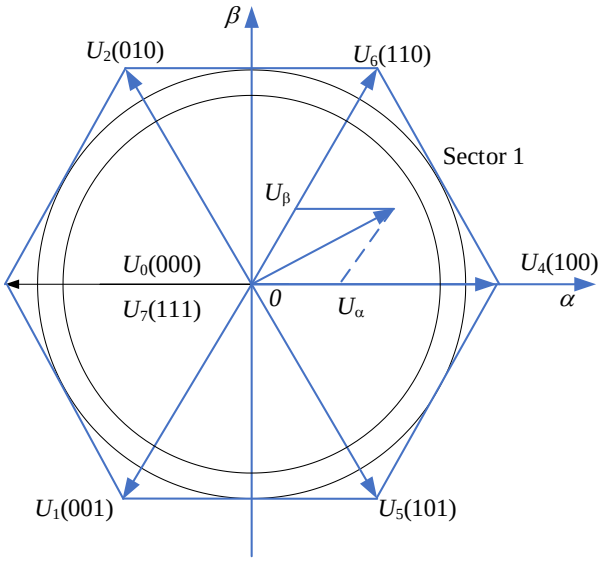

Figure 9. Voltage sector vector diagram

From the voltage space vector diagram, it can be inferred that the Angle between the non-zero voltage vectors is 60°, and they are distributed throughout the plane, dividing the plane into six sectors. For any sector, any vector in the sector can be synthesized by using two non-zero vectors at the boundary of the sector and the corresponding zero vector according to a certain relationship. In this way, any vector in the six sectors can be synthesized. The rotation trajectory of the total voltage synthesized by the three-phase voltage in space is a circle, and any vector rotating along the plane can be synthesized by this method. The specific implementation method is as follows: In the voltage space vector diagram, U_4(100) is selected as the starting position, and a small Angle is selected as the increment, and the target voltage vector is uniformly rotated. The target voltage vector after each increment can be synthesized from the two non-zero vectors and zero vectors in the sector. In this way, when the target voltage vector returns to U_4(100) position again, a trajectory close to the circle can be obtained, so that the idea of SVPWM control can be realized.

Now take the first sector as an example, introduce the formation principle of pulse width modulation waveform in detail, other sectors are similar to the first sector, will not repeat the explanation. Fig. 10 shows the synthesis and decomposition of the target voltage vector in the first sector.

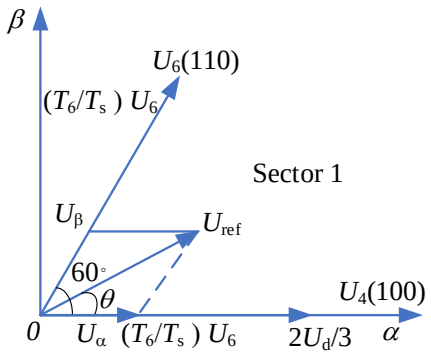

Figure 10. Synthesis and decomposition of the target voltage vector in the first sector

As shown in Figure 2-9, the Angle between the reference voltage vector U_{ref} and U_4 is θ. Now U_{ref} needs to be synthesized by selecting U_4 and U_6 as non-zero vectors and U_0 and U_7 as zero vectors. According to the average value equivalence principle, we can get: Uref Tref=U_4T_4+U_6T_6, where T_{ref}, T_4, and T_6 indicate the total action time, action time of U4, and action time of U6, respectively. Therefore, in the triangle, the sine theorem can list the corresponding expression as shown in formula (10):

$$\frac{|U_{ref}|}{2\pi/3}=\frac{|U_4T_4/T_{ref}|}{\sin(\pi/3-\theta)}=\frac{|U_6T_6/T_{ref}|}{\sin\theta} \tag{10}$$

Since $|U_4|=|U_6|=2V_d/3$, we can get the action time of a nonzero vector as shown in equation (11).

$$\begin{cases} T_4 = pT_{ref}\sin(\pi/3-\theta) \\ T_6 = pT_{ref}\sin\theta \end{cases} \tag{11}$$

Among them, $p = \sqrt{3}\, U_{ref}/V_d$, and action time of zero vector is $T_0 = T_7 = (T_{ref}-T_4-T_6) / 2$.

After determining the time of Uref synthesis in U_4, U_6, U_0 and U_7, it is necessary to consider how to generate the required PWM waveform. In SVPWM control, the zero vector can be selected U_0 and U_7, in general, can be combined with the number of switching actions to determine which zero vector to choose. This is because the switching frequency and the switching loss caused by the switching action change in a positive proportion. Therefore, in order to reduce the switching times of MOS switch, the assignment rule of the basic vector action sequence is set as: only one phase of the three phases is changed each time the switching state is changed. And the zero vector action time is evenly divided to make the generated waveform symmetrical and reduce the harmonic component of the waveform. In the first sector, when switching from U_4 to U_0, only two MOS switches in phase A are switched. If switching from U_4 to U_7, the MOS switches in phase B and C need to be switched at the same time, and the loss will be doubled. Therefore, to switch U_4, U_2, and U_1, work with U_0, and to switch U_6, U_3, and U_5, work with U_7. From this point of view, as long as the switching order in each sector can be determined in advance, the symmetrical PWM waveform of each sector can be derived. Fig. 11 shows the PWM waveforms of the first sector, where T_s is the sampling time.

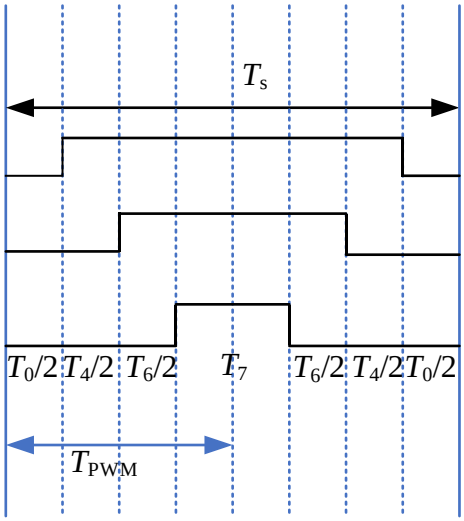

Figure 11. PWM waveforms at first sector

2.4 PRINCIPLE OF ADC CURRENT SAMPLING

When FOC algorithm is applied to motor drive, current sampling must be considered. ADC is a device that converts a continuously varying analog signal into a discrete digital signal. The principle of ADC current sampling is briefly introduced in this part.

Current acquisition circuit is one of the links. Usually, a resistor is used, connected in series to the circuit, and the current flowing through the resistor will form a corresponding voltage; In addition, it can also be converted by current transformer, Hall element and other devices, and the corresponding voltage can also be obtained. This voltage can be easily measured. The acquisition of current is the same as the ADC acquisition of voltage, which requires the hardware to convert the current signal into a voltage signal, and then the ADC is used to collect voltage. First, the ADC is initialized, and then the voltage signal collected by the ADC is converted into a current signal. In current sampling, it should be noted that the sampling resistance should be selected

with high precision and low temperature bleaching resistance to improve the accuracy of the sampling value. In addition, in general, the signal needs to be amplified before collection.

For a three-phase system, the three-phase currents I_a, I_b, and I_c satisfy a mathematical relationship: $I_a+I_b+I_c=0$. Therefore, in order to obtain the three-phase load current of the motor, two of them can be collected to calculate the value of the third term through the above relationship. The ADC of the selected chip can sample two currents at the same time, so that the value of the three-phase phase current can be obtained at the same time after one AD sampling, so which two-phase current should be considered in the application. In the brushless DC motor FOC control technology, the phase current is sinusoidal, so the current to be sampled in different sectors will be different. In the present research, the three phase current of the motor is obtained mainly by the three resistance method. Combined with the three-phase drive voltage waveform, the appropriate current can be selected for each sector for sampling conversion.

3. DESIGN OF FOC SERVO FOR BLDCM CONTROL SYSTEM

Brushless DC motor is developed on the basis of brushless DC motor, with the advantages of endless speed regulation, wide speed regulation range, strong overload capacity, good linearity, long life, small size, light weight, large output, etc., to solve a series of problems existing in brushless motor, widely used in industrial equipment, instrumentation, household appliances, robots, medical equipment and other fields. Because brushless motors do not have brushes for automatic commutation, electronic commutators are needed for commutation. The brushless DC motor driver performs the function of this electronic commutator. Sine-wave control realizes the control of voltage vector and the control of current indirectly, but it cannot control the direction of current. The FOC control mode can be regarded as the upgraded version of sine wave control, which realizes the current vector control, that is, the vector control of the stator magnetic field of the motor. Because the direction of the motor stator magnetic field is controlled, the motor stator magnetic field and the rotor magnetic field can be kept at 90° at all times to achieve the maximum torque output of a certain current. The advantages of FOC control are low torque fluctuation, high efficiency, low noise and fast dynamic response. In order to analyze the feasibility of applying FOC algorithm to DC motor control, the BLDCM servo control system based on FOC algorithm is designed in this chapter.

3.1 CONTROL FLOW OF FOC ALGORITHM

This software system mainly includes the following functions:

(1) Sampling of bus current: This thesis adopts the method of single resistance sampling, through the timer at the right time to trigger the internal and external Settings to sample, and according to the size of the current to play a role in protecting the safety of the circuit.

(2) Electrical Angle estimation: By using the observer to estimate the electrical Angle and speed of the current motor, the corresponding parameters are provided for the following coordinate system transformation and speed loop for corresponding calculation.

(3) Transformation of coordinate system: By sampling the bus current, the sampled current is reconstructed, and the reconstructed three-phase current is sent to Clark formula for calculation, and the purpose of decoupling the current is finally achieved, which is convenient for the control of various physical quantities in the following.

(4) Current loop and speed loop: the decoupled three-phase current is compared with the set current value and speed value to calculate the deviation value.

(5) Inverse Park coordinate transformation: the output values of the current loop and velocity loop are transformed from the two-phase rotating coordinate system to the two-phase stationary coordinate system, and the corresponding components V_α and V_β are obtained to facilitate the calculation of the SVPWM algorithm.

(6) Space vector modulation: According to the obtained V_α and V_β components and the corresponding stator current size, the high level time and phase of the six pulse waves of the timer are calculated through the algorithm to generate the corresponding space voltage vector and control the motor rotation.

(7) Input voltage detection: the input voltage value after voltage division is obtained through the voltage division resistor circuit and the voltage follower, according to the calculated input voltage value to determine whether the circuit is in the state of undervoltage or overvoltage, if the corresponding abnormal phenomenon occurs, the corresponding protection mechanism is triggered for safety protection.

Fig. 12 shows the block diagram of the algorithm control flow. The specific FOC algorithm control includes the following steps:

Step1: Sample the three-phase current of the motor to obtain Ia, Ib, Ic
Step2: Obtain Ialfa, Ibeta through Clark transform
Step3: Obtain Ialfa, Ibeta through Park transform to obtain Iq, Id
Step4: Calculate the error of IqId and its set value Iq_ref Id_ref
Step5: Input the above error into two PID controllers to obtain the output control voltage Uq, Ud
Step6: Perform the inverse Park transformation of Uq, Ud to obtain Ualfa, Ubeta
Step7: The voltage space vector is synthesized with Ualfa, Ubeta, the SVPWM module is input for modulation, and the state code value of the three half-bridges at the moment is output
Step8: The MOS switch of the three-phase inverter is controlled according to the previous output code value, and the motor
Step9: Cycle

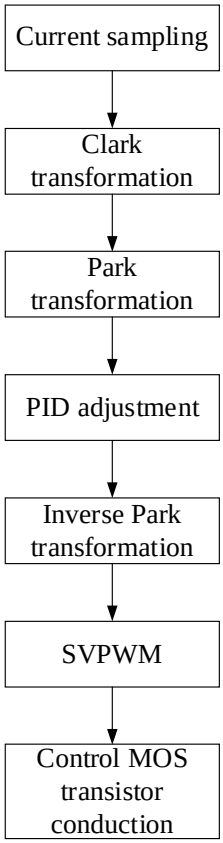

Figure 12. Algorithm control flow diagram

3.2 DESIGN OF THE HARDWARE IN THE SYSTEM

In the hardware operation of BLDCM system, the main control chip, as the carrier of FOC algorithm, plays an important role. Therefore, we should first consider the selection of the main control chip, as the main control chip of the motor, it should have

the analog to digital conversion ability to meet the accuracy requirements, to collect the voltage and current analog signal that reflects the normal operation of the motor, enough to use the interrupt system, can carry out DMA data transmission, has a high frequency of operation speed, can carry out high-speed digital processing, and can be used. High processing capacity, able to complete all the specified operations within the specified time. At the same time, the master chip also needs to send the control signal such as the SVPWM pulse signal obtained by the operation to the driver chip of the switch bridge arm, so as to realize the control of the basic functions of the positive and negative rotation, speed, start and stop of the motor. Combined with the above requirements for microcontrollers, it can be seen that high-speed digital processing and computing capabilities are crucial, and only on this basis can complex signals and operations be processed in a short time. Through comparison and screening, the control device of this driver selects the STM32 Nucleo development board produced by ST Company as the main control board of the whole system.

In order to make BLDCM operate stably under the action of FOC algorithm and adjust its angle, the design block diagram of the whole process is given in the Fig. 13. The main hardware components of the system are as follows: BLDCM DJI 2312, independent AC and DC power conversion circuit, IPM power chip, peripheral circuit of controller, adjustable step-down voltage regulator power module, STM32 development board, downloader and some necessary protection circuit parts. Among them, the selected BLDCM has its own encoder, IPM power chip is an intelligent power module, and the internal integrated three-phase inverter bridge is IGCMF15F60GA. The maximum DC bus voltage can be attached to 450V, the maximum continuous output current is 15A, and the required gate drive voltage is 15V.

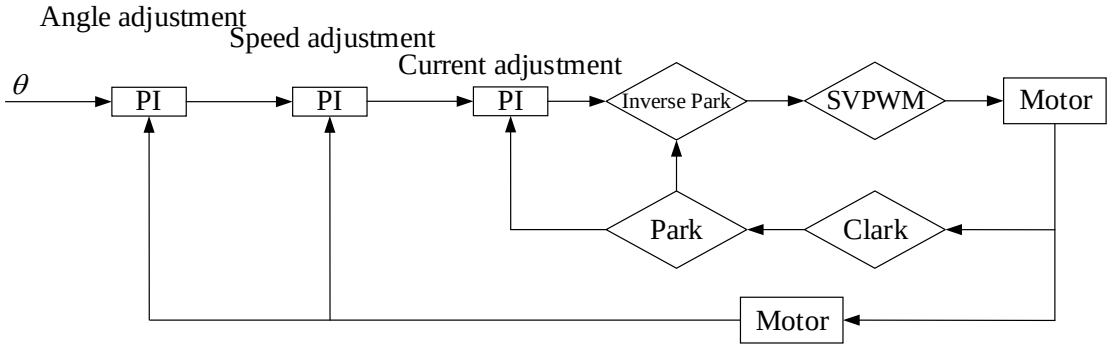

Figure 13. Block diagram of FOC control system

3.3 DESIGN OF IGCMF15F60GA MINIMUM SYSTEM

IGCMF15F60GA minimum system module design plays the most important role in the whole control system design, in addition to the core control chip IGCMF15F60GA, there are circuits to achieve different functions, such as filtering circuits. Fig. 14 is the circuit schematic of IGCMF15F60GA minimum system

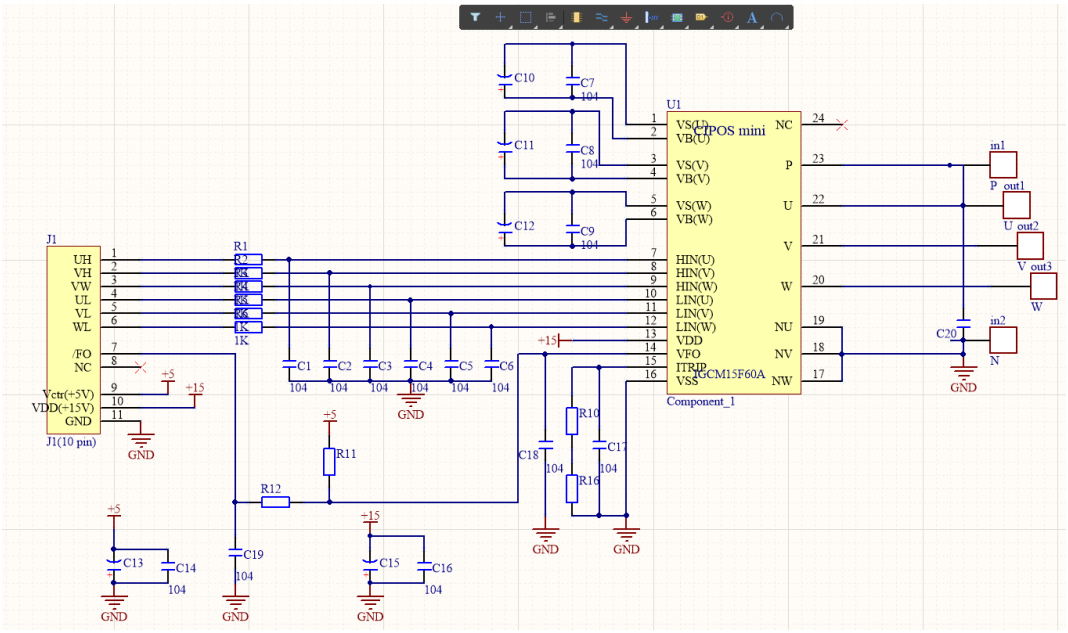

Figure 14. Circuit schematic of IGCMF15F60GA minimum system

In this paper, IGCMF15F60GA, which has excellent performance among IPM power chips, is selected as the main control chip of the control system. Figure 3.3 is the schematic diagram of its minimum system circuit, including the pin arrangement and some parameters, and the operating voltage is 5V, 15V and 24V. In addition, the control chip can process data quickly and bring convenience to the modular design of the control system. Tab. 1 describes the power chip parameters. Fig. 15 shows the equivalent circuit of the power chip.

Table 1. Power chip parameters

Inverter Section

Description	Condition	Symbol	Value		Unit
			min	max	
Max. blocking voltage	I_C = 250µA	V_{CES}	600	-	V
DC link supply voltage of P-N	Applied between P-N	V_{PN}	-	450	V
DC link supply voltage (surge) of P-N	Applied between P-N	$V_{PN(surge)}$	-	500	V
Output current	T_C = 25°C, T_J < 150°C T_C = 100°C, T_J < 150°C	I_C	-10 -6	10 6	A
Maximum peak output current	less than 1ms	$I_{C(peak)}$	-20	20	A
Short circuit withstand time[1]	V_{DC} ≤ 400V, T_J = 150°C	t_{SC}	-	5	µs
Power dissipation per IGBT		P_{tot}	-	26.1	W
Operating junction temperature range		T_J	-40	150	°C
Single IGBT thermal resistance, junction-case		R_{thJC}	-	4.79	K/W

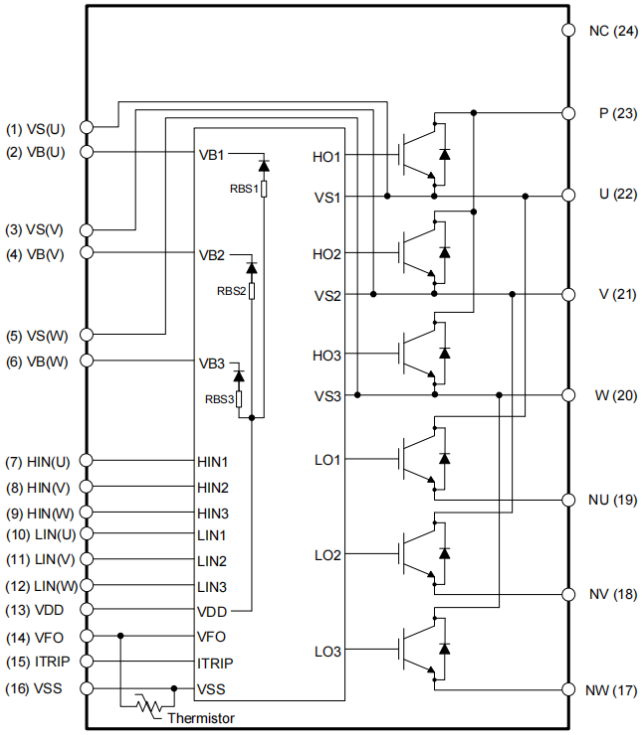

Figure 15. Circuit schematic of IGCMF15F60GA minimum system

HIN(U, V, W) and LIN(U, V, W). These pins are positive logic and are responsible for controlling the integrated IGBT. Their Schmidt trigger input thresholds guarantee LSTTL and CMOS compatibility up to 3.3V controller output. During power start-up, a pull-down resistor of about 5kΩ is provided internally to pre-bias the input, and a Zener clamp is provided to protect the pins. Input Schmitt triggers and noise filters provide beneficial noise suppression for short input pulses. Noise filters suppress control pulses below filter time.

The VDD is the control power supply, which supplies the input logic and the output power level. Input logic reference VSS ground. When the supply voltage is at least a typical voltage of 12.1V, the undervoltage circuit causes the device to operate when powered on. When the VDD supply voltage is low by 10.4V, turn off the power output of all gate drivers. This prevents the external power switch from experiencing severe low gate voltage levels during on-off, thereby preventing excessive power dissipation.

VB(U, V, W) and VS(U, V, W). VB to VS is the high voltage side supply voltage. The high-end circuit can float relative to the VSS, following the emitter voltage of the external high-end power device. Due to low power consumption, the floating driver stage is provided by an integrated bootstrap circuit. The power supply threshold for the undervoltage detection operation rises to a typical value of 12.1V and a descending threshold of 10.4V. VS has high stability against transient negative VSS voltages of -50V. This ensures a very stable design even under rough conditions.

PCB design during the test was drawn based on Altium Designer software. In the physical PCB design, in addition to considering the connection problem of the device interface, it is necessary to take into account the layout of the components, the heat dissipation of the board, the layout of the signal line and the power line and the corresponding electromagnetic compatibility, etc., and pay attention to the following issues:

(1) The layout of the components: The layout of the components largely determines the wiring of the later components. The layout of components should first pay attention to the power circuit device and the control signal device can not be too close to prevent the power signal from interfering with the control signal. At the same time, devices with the same function and electrical connection should be placed together as far as possible, and attention should also be paid to the influence between various components, which can ensure that the lead is shorter in the later period of wiring and reduce the possibility of interference in the middle signal. Finally, the layout of the components should take into account heat dissipation, aesthetics and compactness. Therefore, the layout of components has a great role in the later wiring.

(2) The wiring of the device: The wiring of the device should be strictly planned. There are generally analog signals, digital signals, power supplies, digital ground and analog ground on a board, and there will be a difference between high frequency, medium frequency and low frequency in the signal line. In the face of so many lines, the basic wiring principles are:

(i) For the circuit diagram that requires double-sided wiring, the front and back wires should be kept vertical, oblique or curved wires as far as possible, and parasitic coupling should be avoided after the front and back wires are parallel to each other.
(ii) The corner of the line should be greater than 90 degrees as far as possible, and the corner below 90 degrees should be eliminated. For high-frequency signals, it is necessary to replace it with an arc.
(iii) For high-frequency signals, it is necessary to ensure that the difference in the length of the signal is not large, otherwise, the corresponding wire should be bent and processed to avoid the difference in the transmission of high-frequency signals.
(iv) The signal line should be used as little as possible through the hole and jumper, pay attention to the isolation of the signal line and the power line.
(v) For the power line with high current, it is necessary to widen the line width to avoid the occurrence of serious heating or even wire break due to the thin and narrow copper foil that cannot withstand high current; The floor is very important for the analog circuit, and the noise on the ground may have an inestimable effect on the amplifier circuit. Therefore, it is also necessary to pay attention to electromagnetic compatibility when paving the ground.

(3) Finally, adjust and improve the text and individual components. It is also necessary to check the network relationship of the board to avoid the wrong network relationship caused by minor errors in schematic drawing. Based on the above analysis, the PCB design is finally completed. Fig. 16 shows the PCB circuit board layout diagram of the corresponding design scheme.

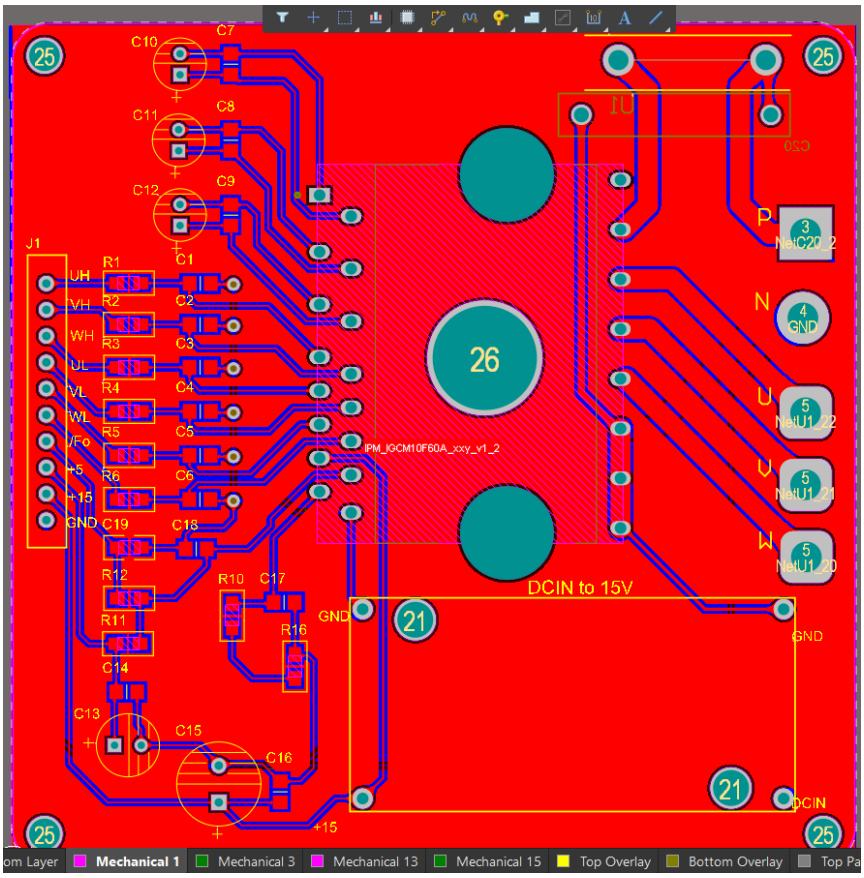

Figure 16. The PCB circuit board layout diagram

3.4 DESCRIPTION OF CONTROL SYSTEM

In order to make the control system work stably, it is particularly important to provide a continuous and stable working power supply for the related devices and circuits in the control system, which mainly requires three different sizes of power supply voltages: 5V, 15V and 24V. The main controller needs +5V DC power supply when it works normally, the IPM power chip needs +15V DC power supply when it works normally, and the +24V power supply is the voltage value required for the normal operation of the brushless DC motor.

Fig. 16 is the corresponding control circuit block diagram as follows, which is mainly composed of the motor control algorithm and PWM modulation. The function is to output 6 PWM signals and control the on-off of the switching tube. The main circuit is composed of three bridge switching circuits and energy storage capacitors, which is responsible for the conversion of DC and AC power.

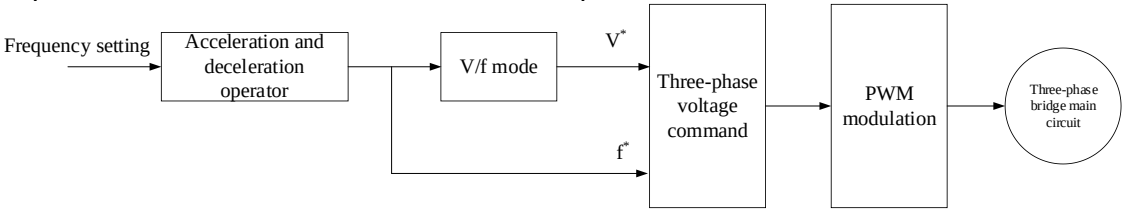

Figure 17. The control circuit block diagram

3.5 DESIGN OF THE SOFTWARE IN THE SYSTEM

3.5.1 DEVELOPMENT TOOL

STM32CubeMX is a graphical tool and configuration and initialization C code generation (STM32 configuration and initialization C code generation), which can automatically generate some of the initial development of the chip related initialization code. It contains all the STM32 series of chips, including the code layer, the intermediate component layer, the hardware abstraction layer a total of three layers.

The STM32CubeMX features are outstanding: It can intuitively select the type of STM32 microcontroller used, and use graphical configuration when configuring the controller, which is clear. C code engineering generator covers STM32 microcontroller initialization compilation software, such as IAR, KEIL, GCC, etc. Here I use KEIL V5. The STM32CubeMX is ST ST's active original tool, which greatly reduces our development time and expense. The STM32CubeMX integrates a comprehensive software platform that supports MCU development for each family of STM32. This platform includes STM32Cube HAL. Plus a compatible set of middleware (RTOS, USB, TCP/IP, and graphics).

In October 2013, Keil launched Keil MDK v5, which uses the uVision5 IDE integrated development environment and is currently the best integrated development tool for ARM microcontrollers, especially ARM Cortex-M core microcontrollers. MDK v5 is divided into two main parts, MDK Core and Software packs. MDK Core is the MDK core, which contains all the components of microcontroller development, including the IDE(uVision5), the editor, the ARM C/C++ editor, the uVision debug tracker, and the Pack Installer. Software packs are MDK software packages, which are divided into three parts: Device, CMSIS, MDK Professional Midleware, and contain various available device drivers.

3.5.2 CORE FUNCTIONS OF FOC

The core function of FOC is to output the desired PWM waveforms after input Ud, Uq and electrical angle.
The specific codes are shown below.

```
void setPhaseVoltage(float Uq, float Ud, float angle_el)
{
   float Uref;
   uint32_t sector;
   float T0,T1,T2;
   float Ta,Tb,Tc;
   float U_alpha,U_beta;
 // Inverse park transformation
   angle_el = _normalizeAngle(angle_el);
   U_alpha=Ud*_cos(angle_el)-Uq*_sin(angle_el);
   U_beta=Ud*_sin(angle_el)+Uq*_cos(angle_el);

   Uref=_sqrt(U_alpha*U_alpha + U_beta*U_beta) / voltage_power_supply;
  //The maximum undistorted rotating voltage vector of SVPWM is the tangent circle of the regular hexagon i.e √3/3=0.577
   if(Uref> 0.577)Uref= 0.577;                                    if(Uref<-0.577)Uref=-0.577;
  // Standardized electrical angle values [0,2pi],+PI/2 is the position of the reference voltage vector
   if(Uq>0)
```

```
        angle_el = _normalizeAngle(angle_el+_PI_2);          else
            angle_el = _normalizeAngle(angle_el-_PI_2);
      sector = (angle_el / _PI_3) + 1; // Determine the sector where the reference voltage resides based on the angle
    // Calculate the action time of two adjacent voltage vectors
      T1 = _SQRT3*_sin(sector*_PI_3 - angle_el) * Uref;      T2 = _SQRT3*_sin(angle_el - (sector-1.0)*_PI_3) * Uref;
      T0 = 1 - T1 - T2;   // Zero vector action time
    // calculate the duty cycles(times)
      switch(sector)
      {
          case 1:
              Ta = T1 + T2 + T0/2;
              Tb = T2 + T0/2;
              Tc = T0/2;
              break;
          case 2:
              Ta = T1 +  T0/2;
              Tb = T1 + T2 + T0/2;
              Tc = T0/2;
              break;
          case 3:
              Ta = T0/2;
              Tb = T1 + T2 + T0/2;
              Tc = T2 + T0/2;
              break;
          case 4:
              Ta = T0/2;
              Tb = T1+ T0/2;
              Tc = T1 + T2 + T0/2;
              break;
          case 5:
              Ta = T2 + T0/2;
              Tb = T0/2;
              Tc = T1 + T2 + T0/2;
              break;
          case 6:
              Ta = T1 + T2 + T0/2;
              Tb = T0/2;
              Tc = T1 + T0/2;
              break;
          default:  // possible error state
              Ta = 0;
              Tb = 0;
              Tc = 0;
      }
    // Output PWM function, configure duty cycle
      __HAL_TIM_SET_COMPARE(&htim1,TIM_CHANNEL_1,Ta*PWM_Period);
      __HAL_TIM_SET_COMPARE(&htim1,TIM_CHANNEL_2,Tb*PWM_Period);
      __HAL_TIM_SET_COMPARE(&htim1,TIM_CHANNEL_3,Tc*PWM_Period);
    }
```

3.5.3 MAIN FUNCTION PART

During the debugging process, sometimes the motor does not react after starting, and

after analysis, it is the reason for the initial position when powering on. In general, the position where the magnetic pole direction of the rotor coincides with the positive direction of alfa is called the zero position of the rotor, that is, the Angle of the rotor at this position is 0°. At this point, the initial value of the power-on encoder is 0. Assuming that when powered on, the position of the rotor is reconnected with the beta axis, in the case of no calibration of the electromechanical Angle, the controller does not know that the position Angle of the rotor is 90°, and the default is 0°, so a Q-axis current of the same position as the rotor will be generated, in this case, the motor will be directly stuck. Therefore, a function to calibrate the initial Angle is added to the main function. When calibration, a current in the direction of alfa is given, and the motor is adsorbed on the alfa axis, and the electrical Angle is the amount of drift required for the target.

```
for(int i=0; i<100;i++)
        {
                setPhaseVoltage(0,2,0);
        }
```

In addition, during the detection, it is found that there are a lot of high-frequency noise interference experiment, and low-pass filtering is added to the main function.

```
float LPF_velocity(float x)
{       float y = 0.9*y_vel_prev + 0.1*x;

        y_vel_prev=y;

        return y;       }
```

The last is the function of PID control for the motor.

```
float PID_angle(float error)
{
        float output,output_ang_prev;
        float proportional,integral,derivative;
        float error_ang_prev;

        proportional = KP_ang * (error);
        integral = integral_ang_prev + KI_ang*Ts*error;
        derivative = KD_ang*(error - error_ang_prev)/Ts;

        output = proportional + integral + derivative;
        output = _constrain(output, -speed_limit, speed_limit);

        integral_ang_prev = integral;
        output_ang_prev = output;
        error_ang_prev = error;

        return output;
}
```

Output PWM function, where vel_LPF is the actual motor speed, calculated by difference of angle.

```
angle=bsp_as5600GetAngle();
        angle_el=angle*7;
        vel_sp=PID_angle(angle_sp-angle);
```

```
Uq_set = PID_velocity(vel_sp-vel_LPF);
setPhaseVoltage(Uq_set, 0, angle_el);

angle_c = angle;
vel_c = (angle_c - angle_prev)/Ts;
vel_LPF=LPF_velocity(vel_c);
angle_prev = angle_c;
```

4. EXPRIMENTAL RESULTS AND ANALYSIS

In the previous chapter, the design of related software algorithm based on FOC control is mainly introduced. However, any motor control system, in addition to software, must also have the corresponding hardware environment to run. Therefore, this chapter will analyze the hardware system environment corresponding to BLDCM. After completing the debugging of BLDCM control system, it is necessary to evaluate the quality of the system. This chapter mainly tests three basic performance indexes of the system, including the test of speed loop response bandwidth, the test of recovery time and the test of speed fluctuation.

4.1 EXPERIMENTAL PRINCIPLE AND PROCESS

The overall hardware structure of BLDCM is mainly composed of power supply circuit, drive circuit, phase current detection circuit, position detection circuit, etc. Fig. 17 is the corresponding hardware structure topology block diagram. Because the BLDCM to be tested uses FOC algorithm, its core technology is SVPWM control. Ignoring the coordinate transformation theory applied to the dq axis for the time being, the basic working principle of the system is that the SVPWM control algorithm and the advanced timer in the main control chip work together to produce 6-channel PWM waveform, and then the 6-channel PWM signal drives the six transistors in the three-phase full-bridge circuit respectively, and then the motor is commutated normally. The position information of the motor rotor is detected by the Hall sensor, and then the speed of the motor is calculated by the capture function of the timer in the main control chip as the feedback speed. The deviation of feedback speed and reference speed is adjusted by PID regulator to get the reference value of current. The phase current of the motor is measured by the resistance method, and the current obtained is the feedback current of the motor. The feedback current is compared with the reference current, and its error is directly applied to the PWM module after adjusting the output of the current PID controller, thus controlling the output of the PWM waveform. In this way, BLDCM speed and current double closed-loop control system can be realized.

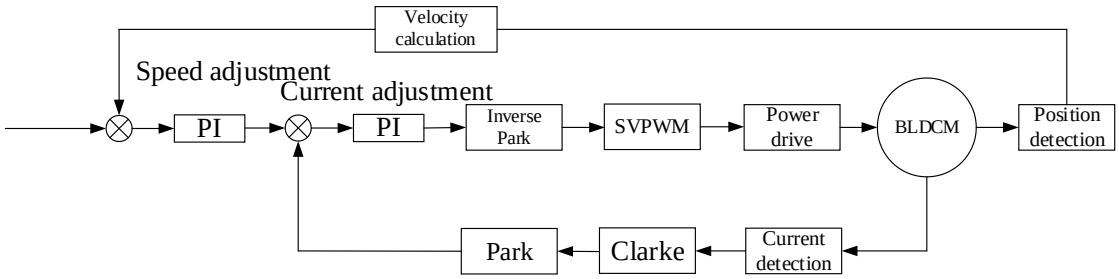

Figure 18. BLDCM hardware structure topology block diagram

First of all, according to the previous design of the hardware module of the control system, the construction of each hardware module is completed, and at the same time, they are connected to a development board in turn according to the direction of signal transmission. Then, through the software design, the motor is driven, and the relevant program flow chart and software code are given. The PID control algorithm is used to adjust and control the speed error of the motor. Finally, in the Keil MDK v5 software environment, the object code is downloaded to the control chip through STLINK. The following is the most important joint debugging of hardware and software, first set up the experimental platform of the entire motor control system, then adjust the software program and observe whether the experimental results achieved the expected effect, and seek a better balance between successful operation and accurate control.

4.2 EXPERIMENTAL PLATFORM

In line with the research background of DC brushless motor speed regulation control system, DJI 2312 motor is selected as the experimental research object. In terms of control strategy, FOC algorithm is adopted to control the generation of three-phase sinusoidal pulse width modulation pulse. The motor speed is controlled by closed-loop control and PID regulator is used to adjust the motor speed. In the hardware design module, the circuit diagram and PCB diagram are drawn by Altium Designer, and then IGCMF15F60GA, which has excellent performance in IPM power chip, is selected as the main controller of the control system, and the related peripheral circuit is designed. Finally, the experimental platform of the whole motor control system is built, and then the hardware and software are debugged jointly to realize the smooth operation of BLDCM driven by FOC algorithm control.

The experimental platform consists of three modules: the physical picture of DJI 2312 brushless DC motor is shown in the Fig. 18, which contains three different colors of leads, which can be directly connected to the corresponding pin of the circuit board (uvw). The circuit board containing the hardware module design of the whole system is shown in the Fig. 19, which is also the most critical part of the whole experiment platform; In addition, there is the STM32 development board and the debugger STLINK V2 that writes programs to the control chip.

After designing the hardware circuit environment of the control system, it is necessary to start debugging the entire control system, so that the brushless DC motor can operate normally under the control system. In the software part, the main is to debug the existing grammar errors, and make corresponding modifications, which is a relatively easy job. More importantly, it is necessary to get the hardware equipment containing the DC motor running. Therefore, it is extremely important to debug the algorithm of the motor. The main debugging method is to connect the usb interface of the computer host and the circuit board with the help of the serial port line, and then download the code to the FLASH of the development board, and then start the motor. During the operation of the motor, many conditions may occur, such as excessive motor speed fluctuations, blocked rotation, and even the motor may not be able to start. At this time, in addition to checking whether the software design is wrong, it is also necessary to check the hardware circuit including the power connection. During the debugging process, the serial port can be used to print and analyze the main variables, such as the voltage and current of the brushless DC motor. The relevant software can be used to plot and analyze the data, and some real-time monitoring software also can be used to detect changes in some variables during the entire motor operation. In short, the debugging of the control system is very important, which determines whether the control algorithm designed in this paper is feasible. And the completion of the debugging process not only requires solid professional knowledge as a foundation, but also should learn from some debugging experience. The BLDCM control system makes the motor run stably by using the debugging method described above.

Figure 19. The physical picture of BLDCM DJI 2312

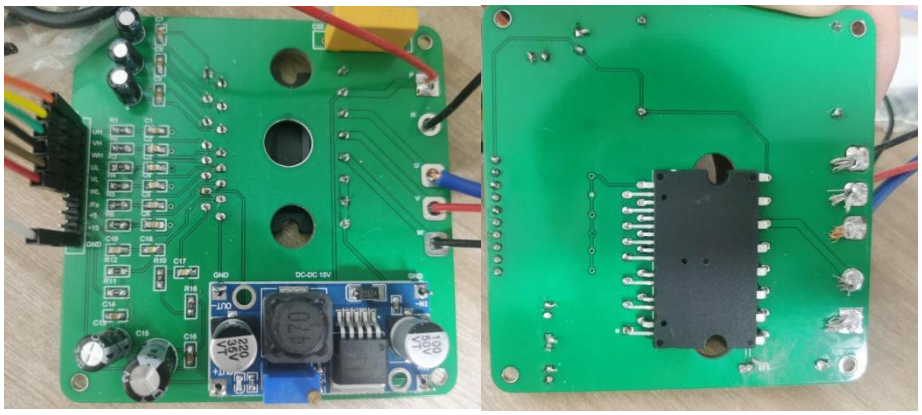

Figure 20. The circuit board containing the hardware module

4.3 FINGDINGS OF EXPERIMENTAL RESULTS

As a summary of the experimental process, in the initial experiment, the adjustable step-down voltage regulator power module welded in the circuit board was short-circuited during the welding process, resulting in the cracking of the capacitor C15, which made me realize that the circuit experiment can only be powered on when all the welding points have been tested intact before the experiment, and later in the design of such experiments, Some protective circuits can be added to prevent further accidents.

According to the requirements of the design, several basic performance indexes of the control system are tested and analyzed, including the speed loop response bandwidth, recovery time and speed fluctuation. According to the needs of these performance indicators, a simple test platform is built, and on the basis of the test platform, each performance indicator is tested and the test results are analyzed. It can be seen that the FOC algorithm can make the motor follow up control more accurately and achieve the expected goal of the proposed control scheme. Through the system-level verification of the improved FOC system, the proper chip and hardware are selected to build a physical platform, and the control effect of the system on BLDCM is actually tested, which proves the correctness and reliability of the system scheme, and completes the important verification link in the chip design.

In general, the simulation and experiment results show that the motor operating state waveform is good, which proves that the scheme has good performance and practicability.

Demo video link：

https://drive.google.com/file/d/1nERvHiFGVq2Xv6A43tRhjApoN2lrCTWP/view?usp=sharing

CONCLUSIONS

In this paper, a three-phase brushless DC motor control scheme based on FOC algorithm is designed, and the specific electrical parameters and control program are given according to the working principle of BLDCM. Finally, the motor drive control is realized. In this paper, according to the current market situation and design requirements, IGCMF15F60GA chip is selected as the microcontrol unit. Aiming at stable and reliable start, low noise, high precision and smooth speed regulation, the related problems in the process of motor start and control operation are analyzed and studied, and the solutions to these problems are given. Through STM32CubeMX, KEIL MDK and other simulation verification methods, as well as the establishment of hardware platform, detailed tests were carried out on each link of the algorithm design, verifying the unity and accuracy of theoretical analysis and design, and completing the overall algorithm design part. The test results show that the FOC algorithm designed in this paper has a good speed regulation effect and meets the needs of motor control in some industrial production. The research of this paper promotes the further development of BLDC control technology, and constructs a BLDC control system with lower cost and more stable performance, which plays a positive role in promoting the BLDC application technology level in industry, transportation and other fields. The work completed in this paper is summarized in the following parts:

(1) By referring to a large number of Chinese and English references, this paper summarizes the cutting-edge technology and research hotspots of the motor control system, conducts a comprehensive research and analysis on the origin of the motor, the development history of the controller and the general situation of the motor control strategy. In order to achieve the servo control of the motor, the FOC algorithm is used in this project to output sine wave to drive the motor control system. The Angle position information of motor is obtained by encoder.

(2) The core components of the brushless DC motor are introduced, the rotor and stator structure and material selection characteristics of the motor body are introduced, the rotor position detection and the working principle of the electronic commutation circuit are introduced, and the corresponding connecting circuit is built according to the working principle of BLDCM.

(3) The principle and control flow of FOC algorithm are introduced. The coordinate transformation and the analysis and judgment of the sector are explained in detail. In particular, park transform and Clark transform are analyzed in detail, including the related formulas and calculation process are described.

(4) In terms of software design, the features and advantages of the STM32CubeMX integrated development environment are first introduced. The hardware abstraction layer of CubeMX can conveniently select the required pins and automatically generate the initialization program, which greatly simplifies our subsequent code writing work. In addition, the program structure diagram is designed and the realization process is described in detail. At the same time, the main algorithm program function and some relatively important program code in the main function are given, including: duty cycle calculation, electrical angle calibration, speed measurement, etc. The pulse width modulation principle of motor control is introduced, and the program code of PWM pulse output is given. Finally, the realization of lower closed-loop control and PID algorithm is introduced, and then all the designed hardware circuits and hardware devices are connected according to the sequence of signals, and the design and welding of the entire BLDCM hardware circuit is completed, including: The circuit module of IGCMF15F60GA minimum system, the circuit module of power supply circuit

and the encoder module of real-time detection of rotor position information play the role of core control. After the experimental platform was built, the KEIL MDK V5 debugger was used to download the compiled program code to the control chip through STLINK V2, and finally the motor was tested to be able to follow up control according to the plan.

The test results show that it is feasible to use the FOC algorithm as the brushless DC motor servo control scheme, the control precision of the brushless DC motor is improved, and the motor fluctuation and noise intensity are suppressed to a certain extent. The brushless DC motor designed and realized in this paper is driven by FOC algorithm to achieve a servo control system, which is completed smoothly. Under the control of the algorithm, the output of the brushless DC motor can be started smoothly, and the speed of the motor can be adjusted without pole or the angle of the electric machine can be locked while the servo control is completed, and the automatic reset can be achieved when external forces are applied. In addition, in the experiment, the noise generated by the motor is very small, and the one-to-many control makes it more suitable for a wide range of applications in factory production and residential life.

Based on FOC control technology, this paper analyzes and studies the servo control of brushless DC motor in detail. However, considering that vector control is very complex, the proposed scheme still has some shortcomings and needs to be improved in future work, which mainly includes the following three aspects:

(1) In terms of algorithm, we should consider the optimization of the existing coordinate transformation and PI controller, and improve the optimization strategies of voltage feedforward compensation and angle compensation to optimize the control performance of the BLDCM system.
(2) There is still room for improvement in the testing process of the control system. It is necessary to further improve the parameters of the current PID regulator and the speed PID regulator in the test system, and optimize the test process, so as to test the three indexes of the speed loop response bandwidth, recovery time and speed fluctuation of the control system, and get more accurate test results.
(3) The PID control algorithm in the proposed scheme is relatively conventional. In order to further improve the operating stability and the rapidity of the response of the DC motor, the direction of the PID control algorithm can be further improved to improve the performance of the entire system.
(4) The hardware test platform of the proposed scheme still needs to be further optimized. Considering that the adjustable step-down voltage regulator power module welded in the circuit board during the experiment is prone to short circuit during the test, the corresponding protection circuit should be further considered during the hardware test. In addition, due to the existence of magnetic circuit coupling in the system, the optimal design scheme of electromagnetic shielding should be further studied and considered in future research.

ACKNOWLEDGMENTS

I have received support and encouragement from many people in completing this dissertation, and I would like to express my sincere gratitude to them.

First of all, I would like to thank my supervisor, Professor Ramon Guzman. He has given me selfless guidance and support throughout the research process. His expertise, in-depth thinking, and guidance on research directions have had a profound impact on me, enabling me to overcome difficulties and make progress in my research.

In addition, I would like to thank Professor Yang for the support of laboratory equipment and resources. Thanks to his support and the experimental conditions provided, I was able to conduct experiments and collect data.

Finally, I would like to thank my family and friends. They have always given me selfless support and understanding during this time. Their encouragement and trust in me was the motivation for me to persevere and finish.

Once again, I would like to thank all the people who have supported and helped me, and your contributions were crucial for me to complete this thesis.

BIBLIOGRAPHY

[1] Kim T , Lee H W , Ehsani M .Position sensorless brushless DC motor/generator drives: review and future trends[J].Electric Power Applications Iet, 2007, 1(4):557-564.DOI:10.1049/iet-epa:20060358.Kim, T., H.W. Lee and M. Ehsani, Position sensorless brushless DC motor/generator drives: Review and future trends. IET Electric Power Applications, 2007. 1(4): p. 557-564.
[2] T. M. Jahns, R. C. Becerra and M. Ehsani, "Integrated current regulation for a brushless ECM drive," in IEEE Transactions on Power Electronics, vol. 6, no. 1, pp. 118-126, Jan. 1991, doi: 10.1109/63.65010.
[3] B. Singh and S. Singh, "State-of-Art on Permanent Magnet Brushless DC Motor Drives," Journal of Power Electronics, vol. 9, no. 1, pp. 1-17, 2009. DOI: 10.6113/JPE.2009.9.1.1.
[4] R. J. Hamilton, "DC motor brush life," in IEEE Transactions on Industry Applications, vol. 36, no. 6, pp. 1682-1687, Nov.-Dec. 2000, doi: 10.1109/28.887222.
[5] Y. B. Li, S. L. Ho, W. N. Fu and B. F. Xue, "Analysis and Solution on Squeak Noise of Small Permanent-Magnet DC Brush Motors in Variable Speed Applications," in IEEE Transactions on Magnetics, vol. 45, no. 10, pp. 4752-4755, Oct. 2009, doi: 10.1109/TMAG.2009.2024882.
[6] Y. Hayashi, H. Mitarai and Y. Honkura, "Development of a DC brush motor with 50% weight and volume reduction using an Nd-Fe-B anisotropic bonded magnet," in IEEE Transactions on Magnetics, vol. 39, no. 5, pp. 2893-2895, Sept. 2003, doi: 10.1109/TMAG.2003.815739.
[7] A. Dimri, R. D. Kulkarni, S. R. Gurumurthy and J. Nataraj, "Design and Simulation of Sensorless Control Algorithms of Brushless DC Motor: A Review," 2018 2nd IEEE International Conference on Power Electronics, Intelligent Control and Energy Systems (ICPEICES), Delhi, India, 2018, pp. 948-952, doi: 10.1109/ICPEICES.2018.8897324.
[8] H. Toda, K. Senda and M. Ishida, "Effect of material properties on motor iron loss in PM brushless DC motor," in IEEE Transactions on Magnetics, vol. 41, no. 10, pp. 3937-3939, Oct. 2005, doi: 10.1109/TMAG.2005.854977.
[9] Furuhashi, T., Sangwongwanich, S., and Okuma, S.: 'A position-and-velocity sensorless control for brushless DC motors using an adaptive sliding mode observer', IEEE Trans. Ind. Electron., 1992, 39, pp. 89– 95.
[10] T. Ishikawa, K. Takahashi, Q. V. Ho, M. Matsunami and N. Kurita, "Analysis of Novel Brushless DC Motors Made of Soft Magnetic Composite Core," in IEEE Transactions on Magnetics, vol. 48, no. 2, pp. 971-974, Feb. 2012, doi: 10.1109/TMAG.2011.2176469.
[11] Y. Liu, J. Zhao, M. Xia and H. Luo, "Model Reference Adaptive Control-Based Speed Control of Brushless DC Motors With Low-Resolution Hall-Effect Sensors," in IEEE Transactions on Power Electronics, vol. 29, no. 3, pp. 1514-1522, March 2014, doi: 10.1109/TPEL.2013.2262391.
[12] S. Sakunthala, R. Kiranmayi and P. N. Mandadi, "A study on industrial motor drives: Comparison and applications of PMSM and BLDC motor drives," 2017 International Conference on Energy, Communication, Data Analytics and Soft Computing (ICECDS), Chennai, India, 2017, pp. 537-540, doi: 10.1109/ICECDS.2017.8390224.
[13] L. Parsa and H. A. Toliyat, "Five-phase permanent-magnet motor drives," in IEEE Transactions on Industry Applications, vol. 41, no. 1, pp. 30-37, Jan.-Feb. 2005, doi: 10.1109/TIA.2004.841021.
[14] Q. Zhang, S. Cheng, D. Wang and Z. Jia, "Multiobjective Design Optimization of High-Power Circular Winding Brushless DC Motor," in IEEE Transactions on Industrial Electronics, vol. 65, no. 2, pp. 1740-1750, Feb. 2018, doi: 10.1109/TIE.2017.2745456.
[15] P. Pillay and R. Krishnan, "Application characteristics of permanent magnet synchronous and brushless DC motors for servo drives," in IEEE Transactions on

Industry Applications, vol. 27, no. 5, pp. 986-996, Sept.-Oct. 1991, doi: 10.1109/28.90357.
[16] C. Xia, Z. Li and T. Shi, "A Control Strategy for Four-Switch Three-Phase Brushless DC Motor Using Single Current Sensor," in IEEE Transactions on Industrial Electronics, vol. 56, no. 6, pp. 2058-2066, June 2009, doi: 10.1109/TIE.2009.2014307.
[17] A. Halvaei Niasar, A. Vahedi and H. Moghbelli, "A Novel Position Sensorless Control of a Four-Switch, Brushless DC Motor Drive Without Phase Shifter," in IEEE Transactions on Power Electronics, vol. 23, no. 6, pp. 3079-3087, Nov.> 2008, doi: 10.1109/TPEL.2008.2002084.
[18] C. -H. Chen and M. -Y. Cheng, "A New Cost Effective Sensorless Commutation Method for Brushless DC Motors Without Phase Shift Circuit and Neutral Voltage," in IEEE Transactions on Power Electronics, vol. 22, no. 2, pp. 644-653, March 2007, doi: 10.1109/TPEL.2006.890006.
[19] J. -X. Shen, S. Cai, D. -M. Miao, D. Shi, J. Gieras and Y. -C. Wang, "Square-wave drive for synchronous reluctance machine and its torque ripple analysis," in CES Transactions on Electrical Machines and Systems, vol. 5, no. 4, pp. 273-283, Dec. 2021, doi: 10.30941/CESTEMS.2021.00032.
[20] J. Shao, "An Improved Microcontroller-Based Sensorless Brushless DC (BLDC) Motor Drive for Automotive Applications," in IEEE Transactions on Industry Applications, vol. 42, no. 5, pp. 1216-1221, Sept.-Oct. 2006, doi: 10.1109/TIA.2006.880888.
[22] R. P. Praveen, M. H. Ravichandran, V. T. Sadasivan Achari, V. P. Jagathy Raj, G. Madhu and G. R. Bindu, "A Novel Slotless Halbach-Array Permanent-Magnet Brushless DC Motor for Spacecraft Applications," in IEEE Transactions on Industrial Electronics, vol. 59, no. 9, pp. 3553-3560, Sept. 2012, doi: 10.1109/TIE.2011.2161058.
[23] D. -K. Hong, B. -C. Woo, D. -H. Koo and U. -J. Seo, "A Single-Phase Brushless DC Motor With Improved High Efficiency for Water Cooling Pump Systems," in IEEE Transactions on Magnetics, vol. 47, no. 10, pp. 4250-4253, Oct. 2011, doi: 10.1109/TMAG.2011.2157482.
[24] Naidu M, Nehl T W, Gopalakrishnan S, et al. Keeping cool while saving space and money: a semi-integrated, sensorless PM brushless drive for a 42-V automotive HVAC compressor[J]. IEEE Industry Applications Magazine, 2005, 11(4): 20-28.
[25] Shao J, Nolan D, Teissier M, et al. A novel microcontroller-based sensorless brushless DC (BLDC) motor drive for automotive fuel pumps[J]. IEEE Transactions on Industry Applications, 2003, 39(6): 1734-1740.
[26] C. C. Chan, J. Z. Jiang, G. H. Chen, X. Y. Wang and K. T. Chau, "A novel polyphase multipole square-wave permanent magnet motor drive for electric vehicles," in IEEE Transactions on Industry Applications, vol. 30, no. 5, pp. 1258-1266, Sept.-Oct. 1994, doi: 10.1109/28.315237.
[27] I. Kawabe, S. Morimoto and M. Sanada, "Output Maximization Control of Wind Generation System Applying Square-Wave Operation and Sensorless Control," 2007 Power Conversion Conference - Nagoya, Nagoya, Japan, 2007, pp. 203-209, doi: 10.1109/PCCON.2007.372968.
[28] J. -X. Shen, S. Cai, D. -M. Miao, D. Shi, J. Gieras and Y. -C. Wang, "Square-wave drive for synchronous reluctance machine and its torque ripple analysis," in CES Transactions on Electrical Machines and Systems, vol. 5, no. 4, pp. 273-283, Dec. 2021, doi: 10.30941/CESTEMS.2021.00032.
[29] G. Griva, T. G. Habetler, F. Profumo and M. Pastorelli, "Performance evaluation of a direct torque controlled drive in the continuous PWM-square wave transition region," in IEEE Transactions on Power Electronics, vol. 10, no. 4, pp. 464-471, July 1995, doi: 10.1109/63.391944.
[30] S. J. Sung, G. H. Jang and H. J. Lee, "Torque Ripple and Unbalanced Magnetic Force of a BLDC Motor due to the Connecting Wire Between Slot Windings," in IEEE Transactions on Magnetics, vol. 48, no. 11, pp. 3319-3322, Nov. 2012, doi: 10.1109/TMAG.2012.2198879.

[31] H. -S. Seol, D. -W. Kang, H. -W. Jun, J. Lim and J. Lee, "Design of Winding Changeable BLDC Motor Considering Demagnetization in Winding Change Section," in IEEE Transactions on Magnetics, vol. 53, no. 11, pp. 1-5, Nov. 2017, Art no. 3101605, doi: 10.1109/TMAG.2017.2695890.D.
[32] Zhao, X. Wang, L. Xu, L. Xia and Y. Huangfu, "A New Phase-Delay-Free Commutation Method for BLDC Motors Based on Terminal Voltage," in IEEE Transactions on Power Electronics, vol. 36, no. 5, pp. 4971-4976, May 2021, doi: 10.1109/TPEL.2020.3039887.
[33] W. -J. Lee and S. -K. Sul, "A New Starting Method of BLDC Motors Without Position Sensor," in IEEE Transactions on Industry Applications, vol. 42, no. 6, pp. 1532-1538, Nov.-dec. 2006, doi: 10.1109/TIA.2006.882668.
[34] K. Kolano, "Improved Sensor Control Method for BLDC Motors," in IEEE Access, vol. 7, pp. 186158-186166, 2019, doi: 10.1109/ACCESS.2019.2960580.
[35] S. Chen, W. Ding, X. Wu, R. Hu and S. Shi, "Novel Random High-Frequency Square-Wave and Pulse Voltage Injection Scheme-Based Sensorless Control of IPMSM Drives," in IEEE Journal of Emerging and Selected Topics in Power Electronics, vol. 11, no. 2, pp. 1705-1721, April 2023, doi: 10.1109/JESTPE.2022.3232410.
[36] H. P, K. Hatua and S. E. Rao, "A Quick Dynamic Torque Control for an Induction-Machine-Based Traction Drive During Square-Wave Mode of Operation," in IEEE Transactions on Industrial Electronics, vol. 69, no. 7, pp. 6519-6529, July 2022, doi: 10.1109/TIE.2021.3095805.
[37] G. Wang, D. Xiao, G. Zhang, C. Li, X. Zhang and D. Xu, "Sensorless Control Scheme of IPMSMs Using HF Orthogonal Square-Wave Voltage Injection Into a Stationary Reference Frame," in IEEE Transactions on Power Electronics, vol. 34, no. 3, pp. 2573-2584, March 2019, doi: 10.1109/TPEL.2018.2844347.
[38] Z. Wang, K. Yu, Y. Li and M. Gu, "Position Sensorless Control of Dual Three-Phase IPMSM Drives With High-Frequency Square-Wave Voltage Injection," in IEEE Transactions on Industrial Electronics, vol. 70, no. 10, pp. 9925-9934, Oct. 2023, doi: 10.1109/TIE.2022.3222683.
[39] D. Zhang, M. Zhou, C. Wang and X. You, "A Single-Current-Regulator Flux-Weakening Control for PMSM Under Square-Wave Mode With Wider Operation Range," in IEEE Transactions on Transportation Electrification, vol. 8, no. 1, pp. 1063-1071, March 2022, doi: 10.1109/TTE.2021.3103270.
[40] F. Zhang, L. Zhu, S. Jin, W. Cao, D. Wang and J. L. Kirtley, "Developing a New SVPWM Control Strategy for Open-Winding Brushless Doubly Fed Reluctance Generators," in IEEE Transactions on Industry Applications, vol. 51, no. 6, pp. 4567-4574, Nov.-Dec. 2015, doi: 10.1109/TIA.2015.2461614.
[41] G. Liu, L. Qu, W. Zhao, Q. Chen and Y. Xie, "Comparison of Two SVPWM Control Strategies of Five-Phase Fault-Tolerant Permanent-Magnet Motor," in IEEE Transactions on Power Electronics, vol. 31, no. 9, pp. 6621-6630, Sept. 2016, doi: 10.1109/TPEL.2015.2499211.
[42] M. Tong, W. Hua, P. Su, M. Cheng and J. Meng, "Investigation of a Vector-Controlled Five-Phase Flux-Switching Permanent-Magnet Machine Drive System," in IEEE Transactions on Magnetics, vol. 52, no. 7, pp. 1-5, July 2016, Art no. 8600105, doi: 10.1109/TMAG.2016.2524503.
[43] W. Zhao, B. Wu, Q. Chen and J. Zhu, "Fault-Tolerant Direct Thrust Force Control for a Dual Inverter Fed Open-End Winding Linear Vernier Permanent-Magnet Motor Using Improved SVPWM," in IEEE Transactions on Industrial Electronics, vol. 65, no. 9, pp. 7458-7467, Sept. 2018, doi: 10.1109/TIE.2018.2795557.
[44] B. Wu, D. Xu, J. Ji, W. Zhao and Q. Jiang, "Field-oriented control and direct torque control for a five-phase fault-tolerant flux-switching permanent-magnet motor," in Chinese Journal of Electrical Engineering, vol. 4, no. 4, pp. 48-56, Dec 2018, doi: 10.23919/CJEE.2018.8606789.
[45] R. Bojoi, P. Guglielmi and G. -M. Pellegrino, "Sensorless Direct Field-Oriented

Control of Three-Phase Induction Motor Drives for Low-Cost Applications," in IEEE Transactions on Industry Applications, vol. 44, no. 2, pp. 475-481, March-april 2008, doi: 10.1109/TIA.2008.916735.
[46] L. Bascetta, G. Magnani, P. Rocco and A. M. Zanchettin, "Performance Limitations in Field-Oriented Control for Asynchronous Machines With Low Resolution Position Sensing," in IEEE Transactions on Control Systems Technology, vol. 18, no. 3, pp. 559-573, May 2010, doi: 10.1109/TCST.2009.2024300.
[47] M. Moallem, B. Mirzaeian, O. A. Mohammed and C. Lucas, "Multi-objective genetic-fuzzy optimal design of PI controller in the indirect field oriented control of an induction motor," in IEEE Transactions on Magnetics, vol. 37, no. 5, pp. 3608-3612, Sept. 2001, doi: 10.1109/20.952673.
[48] Z. Wang, J. Chen, M. Cheng and K. T. Chau, "Field-Oriented Control and Direct Torque Control for Paralleled VSIs Fed PMSM Drives With Variable Switching Frequencies," in IEEE Transactions on Power Electronics, vol. 31, no. 3, pp. 2417-2428, March 2016, doi: 10.1109/TPEL.2015.2437893.
[49] W. Kim, C. Yang and C. C. Chung, "Design and Implementation of Simple Field-Oriented Control for Permanent Magnet Stepper Motors Without DQ Transformation," in IEEE Transactions on Magnetics, vol. 47, no. 10, pp. 4231-4234, Oct. 2011, doi: 10.1109/TMAG.2011.2157956.
[50] M. Jemli, H. B. Azza, M. Boussak and M. Gossa, "Sensorless Indirect Stator Field Orientation Speed Control for Single-Phase Induction Motor Drive," in IEEE Transactions on Power Electronics, vol. 24, no. 6, pp. 1618-1627, June 2009, doi: 10.1109/TPEL.2009.2014867.
[51] Abdelrahem M , Hackl C M , Kennel R .Implementation and Experimental Investigation of A Sensorless Field-Oriented Control Scheme for Permanent-Magnet Synchronous Generators[J].Electrical Engineering, 2017, doi:10.1007/s00202-017-0554-y.
[52] V. Castiglia, P. Ciotta, A. O. Di Tommaso, R. Miceli and C. Nevoloso, "High Performance FOC for Induction Motors with Low Cost ATSAM3X8E Microcontroller," 2018 7th International Conference on Renewable Energy Research and Applications (ICRERA), Paris, France, 2018, pp. 1495-1500, doi: 10.1109/ICRERA.2018.8566749.
[53] W. Li, Z. Xu and Y. Zhang, "Induction motor control system based on FOC algorithm," 2019 IEEE 8th Joint International Information Technology and Artificial Intelligence Conference (ITAIC), Chongqing, China, 2019, pp. 1544-1548, doi: 10.1109/ITAIC.2019.8785597.
[54] G. Bhuvaneswari, B. Singh and S. Madishetti, "Three-phase, two-switch PFC rectifier fed three-level VSI based FOC of induction motor drive," 2012 IEEE Fifth Power India Conference, Murthal, India, 2012, pp. 1-6, doi: 10.1109/PowerI.2012.6479577.